

國立臺灣海洋大學

河海工程學系

碩士學位論文

指導教授：陳正宗 終身特聘教授

邊界積分方程與多極 Trefftz 方法於含圓及球

形邊界 Helmholtz 特徵值問題之研究

A study on eigenproblems for Helmholtz
equation with circular and spherical boundaries
by using the BIEM and the multipole Trefftz
method

研究生：高聖凱 撰

中華民國 98 年 7 月



邊界積分方程與多極 Trefftz 方法於含圓及球形邊
界 Helmholtz 特徵值問題之研究

A study on eigenproblems for Helmholtz equation
with circular and spherical boundaries by using the
BIEM and the multipole Trefftz method

研究生：高聖凱

Student : Shing-Kai Kao

指導教授：陳正宗

Advisor : Jeng-Tzong Chen

國立臺灣海洋大學
河海工程學系
碩士論文

A Thesis
Submitted to Department of Harbor and River Engineering
College of Engineering
National Taiwan Ocean University
In Partial Fulfillment of the Requirements
for the Degree of
Master of Science
in
Harbor and River Engineering
July 2009
Keelung, Taiwan, Republic of China

中華民國 98 年 7 月



誌謝

『心有宏大志，身無逸週時。雖具超聖賦，凱歌仍奏遲。』這是在聽宏治與羿州口試時心裡的寫照，以一個欣賞的角度來看待實驗室同學的口試，除了喜悅之外，心裡卻也有點淡淡的感傷。

進實驗室拜在陳正宗老師門下已經五年了，很感謝老師對我的信任與鼓勵，讓我可以堅持在這條路上走到今天，路途辛苦卻也甘甜。老師努力經營的實驗室真的很棒，非常溫暖與和樂，雖然輝煌的傳統與成績常常會讓人喘不過氣來，不過和這群千金難換的研究伙伴一起同樂，也是我人生難忘的經驗。海洋大學力學聲響振動實驗室（NTOU/MSV）是我另一個家，真的很感謝老師。

感謝口試時，李洋傑老師、呂志宗老師、李為民老師、呂學育老師、岳景雲老師、陳義麟老師、陳桂鴻老師、徐文信老師與范佳銘老師的指正，讓研究可以更加完整，讓我更能體會嚴謹性的重要，未來研究之路還很長，不論是人生與研究，有正確的態度才有完美的結果。

不免俗地感謝研究期間的研究室伙伴。首先感謝阿德學長的無私付出，亦師亦友的身份你扮演得很好；阿夾與羿州兩位研究戰友，一起熬到天亮的伙伴，你們口試表演的很棒，我以你們為榮；魯蛋，小心在研究是嚴謹，但在生活就是龜毛，心寬體胖開朗樂觀的你，別忘了戀愛學分；振鈞、建鋒兩位學弟，謝謝你們幫忙準備的表演舞台，接下來就要看你們表演了；胤祥、文哲與宇志，壓力使人成長，也可以將人擊垮，重點是你如何備戰，跨越你人生的高牆吧。

最後感謝我的家人與女友，研究是需要時間堆疊的，謝謝你們的犧牲與包容，讓我可以無後顧之憂的往前進。謝謝你們包容這樣的我，希望未來的路上，都有你們相伴。另外，感謝國科會 NSC97-2221-E-019-015-MY3 與中興顧問社提供的碩士生獎助學金，有你們的支持讓我無後顧之憂，可以專心於研究。

以幾句話和研究的先進與後輩共勉，

研究點滴在心頭，耕耘幾分又何求？

今朝之景誰能料，後果皆是有前由。

輝煌的背後必然有不為人知的艱辛，耕耘也許無聊枯燥，但突破永遠讓人歡喜不已，研究就是那麼讓人又愛又恨。

A study on eigenproblems for Helmholtz equation with circular and spherical boundaries by using the BIEM and the multipole Trefftz method

Contents

Contents	I
Table captions	III
Figure captions	IV
Notations	VI
Abstract	IX
摘要	X
Chapter 1 Introduction	
1.1 Motivation and literature overview	1
1.2 Organization of the thesis	5
Chapter 2 Eigenproblems with spherical boundaries by using the BIEM	
Summary	11
2.1 Introduction	11
2.2 Null-field integral equation formulation	12
2.2.1 Problem statements	12
2.2.2 Dual null-field integral formulation- the conventional version	13
2.2.3 Dual null-field integral formulation- the present version	14
2.2.4 Expansions of the fundamental solution and boundary density	14
2.2.4.1 Degenerate (separable) kernel for fundamental solutions	15
2.2.4.2 Spherical harmonics for boundary densities	16
2.3 Proof of the existence of spurious eigensolutions for a concentric sphere	16
2.4 Proof the existence for the spurious eigensolutions of the concentric sphere	19
2.5 SVD technique for extracting out true and spurious eigenvalues by using	20

updating terms and updating documents	
2.5.1 Method of extracting the true eigensolutions (updating terms)	20
2.5.2 Method of filtering out the spurious eigensolutions (updating documents)	21
2.6 Illustrative examples and discussions	22
2.7 Conclusions	23
Chapter 3 Eigenproblems with a multiply-connected domain by using the multipole Trefftz method	
Summary	30
3.1 Introduction	30
3.2 Multipole Trefftz method for multiply-connected problems with circular boundaries	32
3.2.1 Problem statement	32
3.2.2 Conventional Trefftz method for the simply-connected domain	32
3.2.3 Graf's addition theorem	33
3.2.4 Multipole Trefftz method	33
3.3 Illustrative examples	36
3.4 Conclusions	38
Chapter 4 Conclusions and further research	
4.1 Conclusions	47
4.2 Further research	48
References	50

Table captions

Table 2-1	Eigensolutions and boundary modes for the concentric sphere subject to different boundary conditions	24
Table 2-2(a)	SVD structure of the four influence matrices for the Dirichlet and Neumann problems in the case of true eigenvalue	25
Table 2-2(b)	SVD structure of the four influence matrices by using the UT singular formulation and LM hypersingular formulation in the case of spurious eigenvalue	26
Table 3-1	The first five eigenvalues for a multiply-connected problem with an eccentric annulus and a concentric annulus using different approaches	39
Table 3-2	The first five modes for a multiply-connected problem with an eccentric hole	40
Table 3-3	The first five modes for a multiply-connected problem with a concentric hole	41
Table 3-4	The first five eigenvalues for a multiply-connected problem with four equal holes using different approaches	42
Table 3-5	The first five modes for a multiply-connected problem with four equal holes	43

Figure captions

Figure 1-1	A brief history of the BEM	7
Figure 1-2	Bump contour	8
Figure 1-3	Limiting process	8
Figure 1-4	Comparison for convergence rate (Hsiao, 2005)	9
Figure 1-5	Mesh generation (Chen and Lee, 2007)	10
Figure 2-1	Sketch of a concentric sphere	27
Figure 2-2	Collocation point on the sphere boundary from the null-field point ($\rho = a^+$)	27
Figure 2-3	Collocation point of the concentric sphere ($\rho = a^-$)	27
Figure 2-4	True eigenvalues for a concentric sphere by using the SVD updating terms ($a = 0.5$ and $b = 1.0$)	28
Figure 2-4(a)	Determinant versus the wave number by using the singular formulation for the Dirichlet condition	28
Figure 2-4(b)	Determinant versus the wave number by using the hypersingular formulation for the Dirichlet condition	28
Figure 2-4(c)	Extraction of true eigenvalues for the Dirichlet problem by using the SVD updating terms	28
Figure 2-4(d)	Determinant versus the wave numbers by using the singular formulation for the Neumann condition	28
Figure 2-4(e)	Determinant versus the wave number by using the hypersingular formulation for the Neumann condition	28
Figure 2-4(f)	Extraction of true eigenvalues for the Neumann problem by using the SVD updating terms	29
Figure 2-5	Extraction of spurious eigenvalues for a concentric sphere by using the SVD updating documents ($a = 0.5$ and $b = 1.0$)	29
Figure 2-5(a)	Determinant versus the wave number by using the singular formulation subject to the Dirichlet condition	29
Figure 2-5(b)	Determinant versus the wave number by using the singular	29

	formulation subject to the Neumann condition	
Figure 2-5(c)	Extraction of the spurious eigenvalues for the singular formulation by using the SVD updating document	29
Figure 2-5(d)	Determinant versus the wave number by using the hypersingular formulation subject to the Dirichlet condition	29
Figure 2-5(e)	Determinant versus the wave number by using the hypersingular formulation subject to the Neumann condition	29
Figure 2-5(f)	Extraction of the spurious eigenvalues for the hypersingular formulation by using the SVD updating document	29
Figure 3-1	A multiply-connected domain with circular boundaries	44
Figure 3-2	Notations of the Graf's addition theorem	44
Figure 3-3	Notations in the multipole Trefftz method	45
Figure 3-4	Determinant versus the wave number by using the multipole Trefftz method for the eccentric case	45
Figure 3-5	Determinant versus the wave number by using the multipole Trefftz method for the concentric case	46
Figure 3-6	Determinant versus the wave number by using the multipole Trefftz method for the multiply-connected case with four equal holes	46

Notations

$P_n^m(\cdot)$	associated Legendre polynomial
$\{u\}, \{t\}$	boundary excitation
B	boundary of a domain
$C.P.V.$	Cauchy principal value
$\{\psi_i\}$	column vector of $[\Psi]$
$\{\phi_i\}$	column vector of $[\Phi]$
D^c	complementary domain
$L^I(s, x)$	degenerate kernel function of $L(s, x)$ for $\bar{\rho} > \rho$
$L^E(s, x)$	degenerate kernel function of $L(s, x)$ for $\rho > \bar{\rho}$
$M^I(s, x)$	degenerate kernel function of $M(s, x)$ for $\bar{\rho} \geq \rho$
$M^E(s, x)$	degenerate kernel function of $M(s, x)$ for $\rho > \bar{\rho}$
$T^I(s, x)$	degenerate kernel function of $T(s, x)$ for $\bar{\rho} > \rho$
$T^E(s, x)$	degenerate kernel function of $T(s, x)$ for $\rho > \bar{\rho}$
$U^I(s, x)$	degenerate kernel function of $U(s, x)$ for $\bar{\rho} \geq \rho$
$U^E(s, x)$	degenerate kernel function of $U(s, x)$ for $\rho > \bar{\rho}$
$[\Sigma]$	diagonal matrix
$\delta(\cdot)$	Dirac-delta function
r	distance between the source point s and the field point x , $r \equiv x - s $
D	domain of interest
x	field point
(ρ, ϕ, θ)	field point in the spherical coordinates
$H.P.V.$	Hadamard (or called Mangler) principal value
H	Hermitian operator
$[\mathbf{I}]$	identity matrix
$[\mathbf{M}]$	influence matrix of the kernel function $M(s, x)$
$[\mathbf{L}]$	influence matrix of the kernel function $L(s, x)$
$[\mathbf{T}]$	influence matrix of the kernel function $T(s, x)$

[U]	influence matrix of the kernel function $U(s, x)$
$L(s, x)$	kernel function in the hypersingular formulation
$M(s, x)$	kernel function in the hypersingular formulation
$T(s, x)$	kernel function in the singular formulation
$U(s, x),$	kernel function in the singular formulation
∇^2	Laplacian operator
ε_m	Neumann factor
N	number of the circular boundaries
\mathbf{n}	normal vector
\mathbf{n}_s	normal vector at the source point s
\mathbf{n}_x	normal vector at the field point x
$t(s)$	normal derivative of $u(s)$ at s
$t(x)$	normal derivative of $u(x)$ at x
(ρ, ϕ)	polar coordinate of x
\mathbf{O}_j	position vector of the j th circular center
(ρ_j, ϕ_j)	position vector of the field point with respect to \mathbf{O}_j
$u(x)$	potential function on the field point x
$u(s)$	potential function on the source point s (on the boundary)
R_j	radius of the j th circular boundary
a, b	radius of a spherical boundary
$R.P.V.$	Riemann principal value
s	source point
$(\bar{\rho}, \bar{\phi}, \bar{\theta})$	source point in the spherical coordinates
A_{vw}^i, B_{vw}^i	sphere coefficient on the i th boundary
$\varphi_m(\cdot)$	T-complete function
$H_n^{(1)}(\cdot)$	the derivative of $H_n^{(1)}(\cdot)$
$h_n^{(2)}(\cdot)$	the derivative of $h_n^{(2)}(\cdot)$
$J_n'(\cdot)$	the derivative of $J_n(\cdot)$
$j_n'(\cdot)$	the derivative of $j_n(\cdot)$
$y_n'(\cdot)$	the derivative of $y_n(\cdot)$

$J_n(\cdot)$	the n th order Bessel function of the first kind
$Y_n(\cdot)$	the n th order Bessel function of the second kind
$H_n^{(1)}(\cdot)$	the n th order Hankel function of the first kind
$j_n(\cdot)$	the n th order sphere Bessel function of the first kind
$y_n(\cdot)$	the n th order sphere Bessel function of the second kind
$h_n^{(2)}(\cdot)$	the n th order sphere Hankel function of the second kind
M	truncated term of the Trefftz bases
A_{vw}	unknown coefficients of boundary density $u(s)$
B_{vw}	unknown coefficients of boundary density $t(s)$
α_m^j	unknown coefficient of the m th complete function for \mathbf{O}_j
$[\Phi], [\Psi]$	unitary matrix
k	wave number
$W(\cdot, \cdot)$	Wronskian property

Abstract

In this thesis, the multipole Trefftz method and the null-field integral equation are employed to deal with 2-D and 3-D eigenproblems, respectively. In the chapter 2, the null-field integral equation in conjunction with degenerate kernels and spherical harmonics are utilized to solve the eigenproblem of a concentric sphere. By expanding the fundamental solution into degenerate kernels and expressing the boundary density in terms of spherical harmonics, all boundary integrals can be analytically determined. By using the updating terms and updating document of singular value decomposition (SVD) technique, true and spurious eigenvalues can be extracted out, respectively. Besides, true and spurious boundary eigenvectors are obtained in the right and left unitary vectors in the SVD structure of the influence matrices. This finding agrees with that of 2-D cases. In the chapter 3, we succeed to extend the conventional Trefftz method to the multipole Trefftz method in eigenproblems. The multipole Trefftz method is used to deal with eigenproblems with a multiply-connected domain. By introducing the addition theorem, the collocation technique is not required to construct the linear algebraic system. The eigenvalues can be found by employing the direct searching technique. Solving eigenproblems by using this method is free of pollution of spurious eigenvalues.

Keywords: degenerate kernel, null-field integral equation, multipole Trefftz method, eigenproblem, spurious eigenvalue

摘要

本文利用多極 Trefftz 方法與零場積分方程，分別處理二維與三維的特徵值問題。在第二章，零場積分方程引入退化核與球形諧和函數解同心圓球的特徵值問題。透過退化核函數展開基本解與利用球形諧和函數表示邊界物理量，則邊界積分便可以解析求得。真假特徵值分別透過奇異值分解的補充列與補充行技巧焯出。此外，真假邊界特徵向量可以在影響係數矩陣的奇異值分解結構中左酉與右酉矩陣的行向量發現。這些發現與二維例子吻合。第三章，在特徵值問題上成功地將傳統 Trefftz 方法推展到多極 Trefftz 方法。利用多極 Trefftz 方法處理多連通定義域的特徵值問題。因為引入了加法定理，所以無須佈點的技巧即可建構出一個線性代數系統。特徵值可以透過直接搜尋的技巧獲得。利用此法解特徵值問題將無假根的污染產生。

關鍵字：退化核、零場積分方程、多極 Trefftz 方法、特徵值問題、假根

Chapter 1 Introduction

1.1 Motivation and literature overview

Acoustic analysis becomes a more and more important issue in new product design process. Many scholars have studied the sound radiation behavior and tried to find the connection between the sound radiation and vibration. Since exact or analytical solutions aren't always available, they aimed to find a numerical approach to decouple the sound radiation. Many well-developed numerical methods such as the finite difference method (FDM), the finite element method (FEM) and the boundary element method (BEM) have been adopted. The FDM approximates the derivatives in the differential equations which govern problems using some types of truncated Taylor expansion and thus express them in terms of the values at a number of discrete mesh points. The main difficulty of this technique is the consideration of curved geometries and the application of boundary condition.

For the case of general boundaries, the regular finite difference grid is unable to accurately reproduce the geometry of the problem. In the past decade, the FEM has been widely applied to carry out many engineering problems. The FEM utilizes a weighted residual method of the minimum potential energy theorem. The disadvantages of the FEM are inconvenient in modeling infinite regions and dealing with quantities of data, especially for three-dimensional problems. The governing equation in BEM is an integral equation different from those in the others. The integral equation was introduced by Fredholm in 1903. The origin of the boundary element method can be traced to the work carried out by some researchers in the 1960's on the applications of boundary integral equations to potential flow and stress analysis problems. In the 1960 period, the BEM was utilized to solve 2-D elasticity by Rizzo (1967) and 2-D elastodynamics problem by Cruse and Rizzo (1968). In 1978, the first book on boundary elements in its title was published (Brebbia, 1978), and the first international conference on the topic was organized. From 1978 to 1986, the mathematical foundation of the BEM is focused on the singular integral equation with the Cauchy kernel. In order to solve the problems with degenerate boundaries, Hong

and Chen (1988) introduced the dual BEM with the hypersingular formulation. Another break through of the BEM is the introduction of degenerate kernels which makes fast multipole BEM possible. A brief history of the BEM is shown in Fig. 1-1. The BEM has become popular in recent years due to its advantage of the reduction of dimensionality. Although the capability of the BEM has been verified for solving engineering problems, there are five critical issues as given below.

(1) Treatment of weak, strong and hypersingular singularities

It's well-known that improper integral should be handled particularly when the BEM is used. In the dual BIEM/BEM formulation, the singular and hypersingular integrals need special care by using the sense of Cauchy and Hadamard principal values (CPV and HPV), respectively. How to determine accurately the free terms had received more attentions in the past decade and a large amount of the papers can be found. Two conventional techniques, bump contour approach (Guiggiani, 1995) and the limiting process (Gray and Manne, 1993) as shown in Figs. 1-2 and 1-3, were employed to regularize the singular and hypersingular integrals. Another alternative to avoid the singularity, such as fictitious BEM and null-field approach (off boundary approach; Achenbach, Kechter and Xu, 1988) can be considered. However, they result in an ill-posed matrix. How to extract principle values of singular and hypersingular integrals using the well-posed model is an interesting object.

(2) Ill-posed model

By moving the null-field points to the real boundary or adjusting the fictitious boundary to the real boundary, the system can be changed to be well-posed. However, CPV and HPV need to be calculated. Instead of determining the CPV or HPV, the kernel function is separable since the double-layer potential is discontinuous across the boundary. Therefore, the degenerate kernel, namely separable kernel, is employed to represent the potential of the perforated domain which satisfies the governing equation.

(3) Boundary-layer effect

Boundary-layer effect in the BEM occurs when the collocation point approaches the vicinity near boundary. Kisu and Kawahara (1988) proposed a concept of relative quantity to eliminate the boundary-layer effect. Chen and Hong in Taiwan (1994) as well as Chen et al. in China (2001) independently extended the idea of relative quantity to two regularization techniques which the boundary densities are subtracted by constant and linear terms. For the stress calculation, Sladek et al. (1991) used a regularized version of the stress boundary integral equation to compute the correct values of stresses close to the boundary. Others proposed a regularization of the integrand by using variable transformations. For example, Telles (1987) used a cubic transformation such that its Jacobian is the minimum at the point on the boundary close to the collocation point and can smooth the integrand. Similarly, Huang and Cruse (1993) proposed rational transformations which regularized the nearly singular integrals. We concern how to develop a BIEM formulation free of boundaries-layer effect.

(4) Convergence rate

The BEM is very popular for boundary value problems with general geometries since it requires discretization on the boundary only. Regarding constant, linear and quadratic elements, the discretization scheme does not take the special geometry into consideration. However, it leads to the slow convergence rate. Convergence rate of exponential order by using the null-field integral equation was achieved as demonstrated by Hsiao (2005). Moreover, the present method can be directly applied to problems with general boundaries without any difficulty once the fundamental solution can be separated in other coordinate system, such as Cartesian coordinates or the elliptic coordinates.

(5) Mesh generation

Although BEM is free of domain discretization, boundary mesh generation is still required since collocation point is on the boundary. We introduce the generalized Fourier coefficients for problems with circular boundaries. Boundary type methods,

the BEM, MFS and Trefftz method, have received more attention in the recent years. In analogy of clinical medicine, the FEM behaves like operation, the BEM is similar to diagnosis by feeling the pulse and boundary collocation method behaves like acupuncture and moxibustion (Chen and Lee, 2007).

For the Helmholtz equations, it is well-known that the complex-valued BEM can determine the eigensolutions by using direct searching scheme (De Mey, 1976). Nevertheless, complex-valued computation is time consuming and not simple. A simplified method using only the real-part or imaginary-part kernel was also presented by De Mey (1977). Although De Mey found the zeros for real-part determinant, the spurious solutions were discovered if only a real-part formulation was employed. Spurious and fictitious frequencies occur and stem from non-uniqueness solution problems. They appear in different aspects on computational mechanics. For example, hourglass modes in the FEM using the reduced integration occur due to the rank deficiency (Winkler and Davies, 1984). Also, loss of divergence-free constraint for the incompressible elasticity results in spurious modes. In the other aspect of numerical solution for the differential equation using the FDM, the spurious eigenvalue also appears due to discretization (Greenberg, 1998; Fujiwara, 2007; Zhao, 2007). If the incomplete set is adopted in the solution representation such as the real-part BEM (Kuo et al., 2000) or MRM (Chen and Wong, 1997; Chen and Wong, 1998; Yeih et al., 1998; Yeih et al., 1999(a)(b); Chen et al., 2003(a)), spurious eigensolutions occur in solving eigenproblems with simply-connected domain. Even though the complex-valued kernel is adopted in the BEM, the spurious eigensolution also occurs for multiply-connected problems (Chen et al., 2003(b)) as well as the appearance of fictitious frequency for exterior acoustics (Chen et al., 2006(a)). Spurious solutions and fictitious frequencies in the integral formulation belong to spectral pollution since it cannot be suppressed by refining the mesh. The origin of spurious modes arises from an improper approximation of null space of the integral operator (Schroeder, 1994). Based on successful experiences, how spurious eigenvalues in 3-D concentric sphere occur is one of our concerns in this thesis. We do not only consider 3-D eigenproblems using BIEM but also focus on finding a

meshless method free of spurious eigenvalue.

In recent years, meshless methods started to capture the interest of the researchers in the community of computational mechanics because these methods are mesh free and only boundary nodes are necessary (Young et al., 2005; Chen et al., 2006(b); Atluri et al., 1999; Atluri and Shen, 2002). Among meshless methods, the Trefftz method is a boundary-type solution procedure using only the T-complete functions which satisfy the governing equation (Li et al., 2008). Since Trefftz presented the Trefftz method for solving boundary value problems in 1926 (Trefftz, 1926), various Trefftz methods such as direct formulations and indirect formulations (Kita and Kamiya, 1995) have been developed. The key issue in the use of the indirect Trefftz method is the definition of T-complete function set, which ensures the convergence of the subsequent field variable expansions towards the analytical solutions. Many applications to the Laplace equation (Karageorghis and Fairweather, 1999), the Helmholtz equation (Fairweather and Karageorghis, 1998), the Navier equation (Jin et al., 1990 and 1993) and the biharmonic equation (Jirousek and Wroblewski, 1996) were done. Readers can consult with Li et al.'s book (Li et al., 2008). However, all the applications seemed to be limited on simply-connected domains. The concept of multipole method to solve exterior problems was firstly devised by Závřiska (1913) and used for the interaction of waves with arrays of circular cylinders by Linton and Evans (1990). Recently, Martin (2006) reviewed several methods to solve problems of the multiple scattering in acoustics, electromagnetism, seismology and hydrodynamics. However, the interior eigenproblems were not mentioned therein. Extension to interior multiply-connected problems by using the multipole Trefftz method is also our concern.

1.2 Organization of the thesis

In this thesis, the multipole Trefftz method and the null-field integral equation are employed to deal with 2-D and 3-D eigenproblems, respectively. The null-field integral equation in conjunction with degenerate kernels and spherical harmonics are utilized to solve the eigenproblem of a concentric sphere. The multipole Trefftz

method is used to deal with eigenproblems with a multiply-connected domain. The organization of each chapter is summarized below.

In the chapter 2, we derive the unified formulation of the null-field integral equation approach for 3-D eigenproblems. By expanding the fundamental solution into degenerate kernels and expressing the boundary density in terms of the spherical harmonics, all boundary integrals can be analytically determined. By using the updating terms and updating document of singular value decomposition (SVD) technique, true and spurious eigenvalues can be extracted out, respectively.

In the chapter 3, we employ the addition theorem to expand the Bessel (J) and Hankel (H) functions (Graf, 1893) in the solution representation for matching the boundary conditions in an analytical way. The so-called multipole Trefftz method is analytical and effective in solving problems with the multiply-connected domain. By introducing the addition theorem, the collocation technique is not required to construct the linear algebraic system. The eigenvalues can be found by employing the direct searching technique. Solving eigenproblems by using this method is free of pollution of spurious eigenvalues. Finally, we draw out some conclusions item by item and reveal some further topics in the chapter 4.

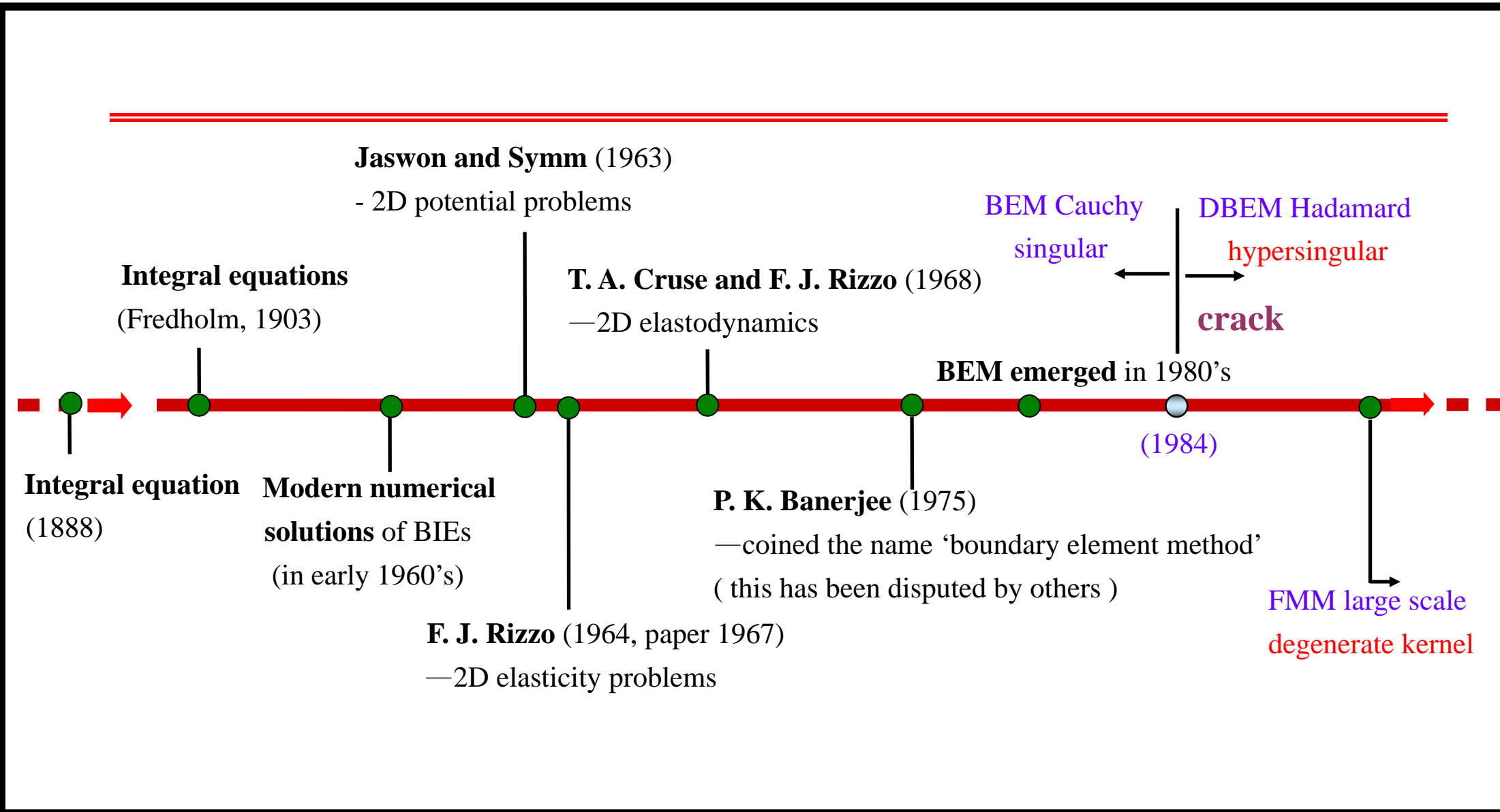


Figure 1-1 A brief history of the BEM

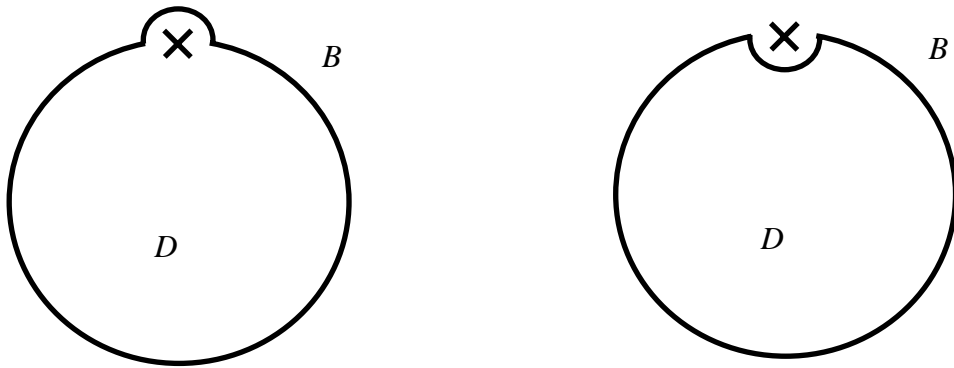


Figure 1-2 Bump contour

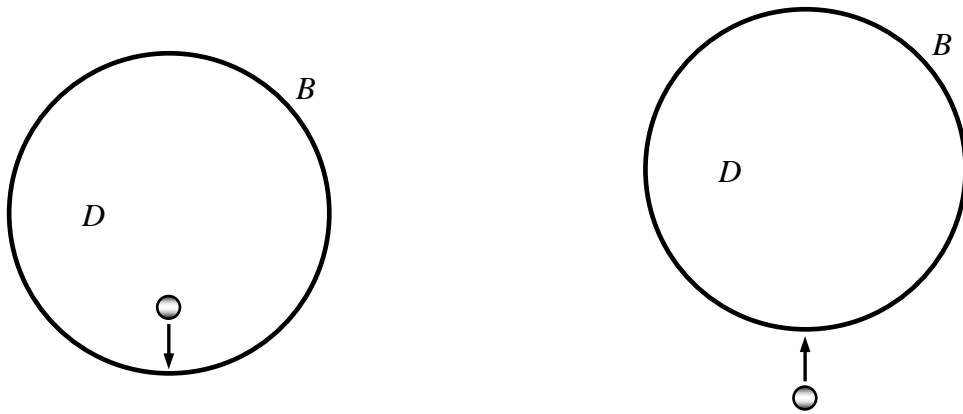


Figure 1-3 Limiting process

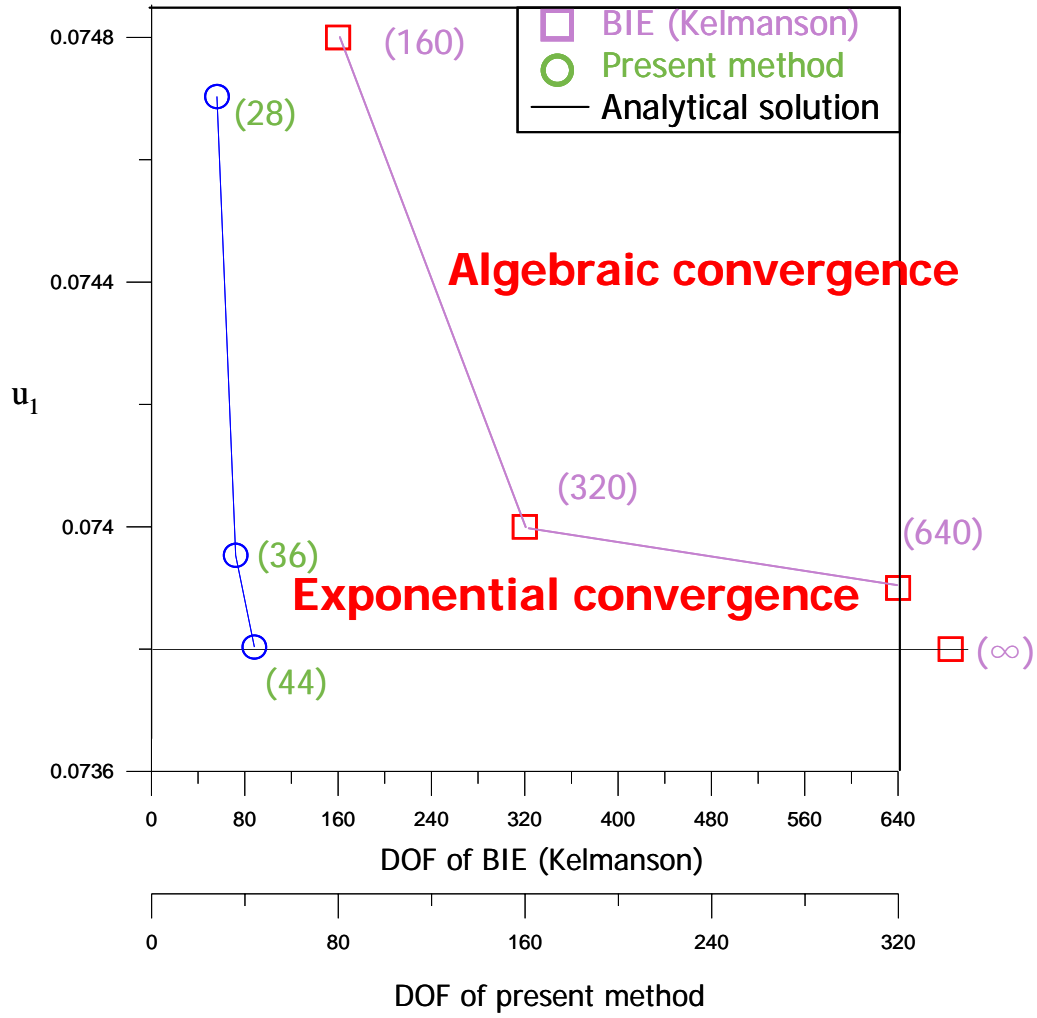


Figure 1-4 Comparison for convergence rate (Hsiao, 2005)

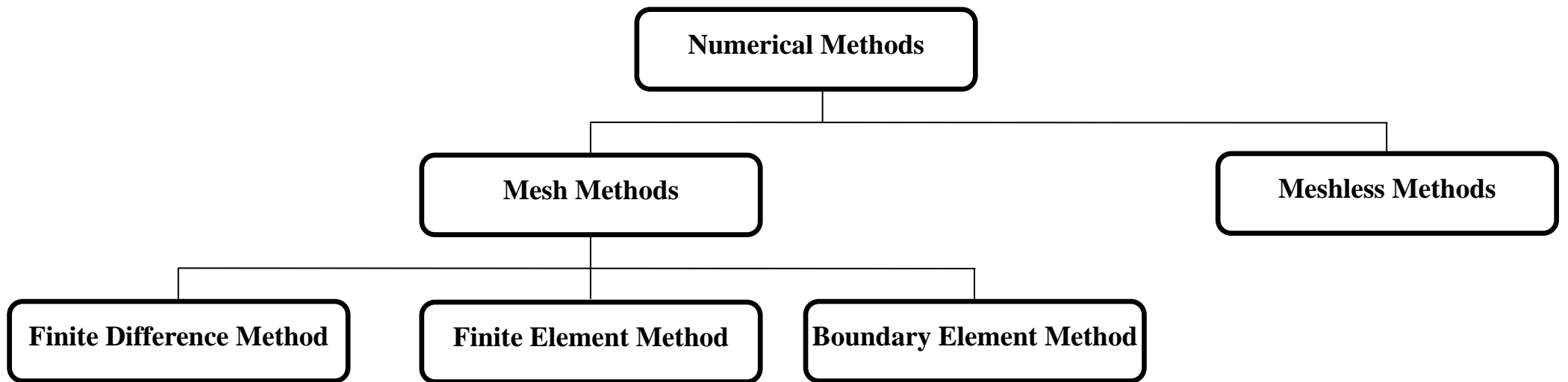


Figure 1-5 Mesh generation (Chen and Lee, 2007)

Chapter 2 Eigenproblems with spherical boundaries by using the BIEM

Summary

In this chapter, the null-field integral equation method is employed to study the occurring mechanism of spurious eigenvalues for a concentric sphere. By expanding the fundamental solution into degenerate kernels and expressing the boundary density in terms of spherical harmonics, all boundary integrals can be analytically determined. It is noted that our null-field integral formulation can locate the collocation point on the real boundary thanks to the degenerate kernel. In addition, the spurious eigenvalues are parasitized in the formulations while true eigensolutions are dependent on the boundary condition such as the Dirichlet or Neumann problem. By using the updating terms and updating document of the SVD technique, true and spurious eigenvalues can be extracted out, respectively. Besides, true and spurious boundary eigenvectors are obtained in the right and left unitary vectors in the SVD structure of the influence matrices. This finding agrees with that of the 2-D cases (Chen et al., 2009).

2.1 Introduction

The application of eigenanalysis is gradually increasing for vibration and acoustics. The demand for eigenanalysis calls for an efficient and reliable method of computation for eigenvalues and eigenmodes. Over the past three decades, several boundary element formulations have been employed to solve the eigenproblems (Ali, Rajakumar and Yunus, 1995), e.g., determinant searching method, internal cell method, dual reciprocity method, particular integral method and multiple reciprocity method. In this chapter, we will focus on the determinant searching method with emphasis on spurious eigenvalues when using the BIEM for 3-D problems with an inner hole. Spurious and fictitious solutions stem from non-uniqueness solution problems which appear in different aspects in computational mechanics. First of all, hourglass modes in the finite element method (FEM) using the reduced integration occur due to rank deficiency (Winkler and Davies, 1984). Also, loss of divergence-free constraint for the incompressible elasticity results in spurious modes. On the other hand, while solving the differential equation by using

the finite difference method (FDM), the spurious eigenvalue also appears due to discretization (Greenberg, 1998; Fujiwara, 2007; Zhao, 2007). In the real-part BEM (Kuo et al., 2000) or the MRM formulation (Chen and Wong, 1997 and 1998; Yeih et al., 1998; Yeih, Chen and Chang, 1999; Yeih et al.(a)(b), 1999; Chen and Kuo, 2003), spurious eigensolutions occur in solving eigenproblems. Even though the complex-valued kernel is adopted, the spurious eigensolution also occurs for the multiply-connected problem (Chen et al., 2001; Chen, Liu and Hong, 2003) as well as the appearance of fictitious frequency for the exterior acoustics (Chen et al., 2006(a)). Spurious eigenvalues in the method of fundamental solutions (MFS) for 3-D problems were also studied by Tsai *et al.* (2006). In this chapter, a simple case of 3-D concentric sphere will be demonstrated to see how spurious eigensolutions occur and how they are suppressed by using SVD.

In the recent years, the SVD technique has been applied to solve problems of fictitious-frequency (Chen et al., 2006(a)) and continuum mechanics (Chen et al., 2002). Two ideas, namely updating term and updating document (Chen et al., 2006(a)), were successfully applied to extract the true and spurious solutions, respectively. In this chapter, the three-dimensional eigenproblem of a concentric sphere is studied in both numerical and analytical ways. Owing to the introduction of degenerate kernel, the collocation point can be located exactly on the real boundary. Besides, true and spurious equations can be found by using the null-field integral equation in conjunction with degenerate kernels and spherical harmonics. Surface distributions of the inner and outer boundaries can be expanded in terms of spherical harmonics. Since a spurious eigenvalue is embedded in the numerical method and has no physical meaning, the remedies, SVD updating term and SVD updating document, are used to extract or filter out true and spurious eigenvalues, respectively. Finally, an example with various boundary conditions is utilized to validate the present approach by using singular and hypersingular formulations.

2.2 Null-field integral equation formulation

2.2.1 Problem statements

The governing equation for the eigenproblem of a concentric sphere is the Helmholtz equation as follows:

$$(\nabla^2 + k^2)u(x) = 0, \quad x \in D, \quad (2-1)$$

where ∇^2 , k and D are the Laplacian operator, the wave number and the domain of interest, respectively. The concentric sphere is depicted in Fig. 2-1. The inner and outer radii are a and b , respectively.

2.2.2 Dual null-field integral formulation — the conventional version

The dual boundary integral formulation (Zhao, 2007) for the domain point is shown below:

$$4\pi u(x) = \int_B T(s, x)u(s)dB(s) - \int_B U(s, x) \frac{\partial u(s)}{\partial n_s} dB(s), \quad x \in D, \quad (2-2)$$

$$4\pi \frac{\partial u(x)}{\partial n_x} = \int_B M(s, x)u(s)dB(s) - \int_B L(s, x) \frac{\partial u(s)}{\partial n_s} dB(s), \quad x \in D, \quad (2-3)$$

where x and s are the field and source points, respectively, B is the boundary, n_x and n_s denote the outward normal vectors at the field point and the source point, respectively, and the kernel function $U(s, x)$ is the fundamental solution which satisfies

$$(\nabla^2 + k^2)U(s, x) = 4\pi\delta(x - s). \quad (2-4)$$

where $\delta(\cdot)$ is the Dirac-delta function. The other kernel functions can be obtained as

$$T(s, x) = \frac{\partial U(s, x)}{\partial n_s}, \quad (2-5)$$

$$L(s, x) = \frac{\partial U(s, x)}{\partial n_x}, \quad (2-6)$$

$$M(s, x) = \frac{\partial^2 U(s, x)}{\partial n_s \partial n_x}. \quad (2-7)$$

If the collocation point x is on the boundary, the dual boundary integral equations for the boundary point can be obtained as follows:

$$2\pi u(x) = C.P.V. \int_B T(s, x)u(s)dB(s) - R.P.V. \int_B U(s, x) \frac{\partial u(s)}{\partial n_s} dB(s), \quad x \in B, \quad (2-8)$$

$$2\pi \frac{\partial u(x)}{\partial n_x} = H.P.V. \int_B M(s, x)u(s)dB(s) - C.P.V. \int_B L(s, x) \frac{\partial u(s)}{\partial n_s} dB(s), \quad x \in B, \quad (2-9)$$

where $R.P.V.$, $C.P.V.$ and $H.P.V.$ are the Riemann principal value, the Cauchy principal value and the Hadamard (or called Mangler) principal value, respectively. By collocating x outside the domain, we obtain the null-field integral equation as shown below:

$$0 = \int_B T(s, x)u(s)dB(s) - \int_B U(s, x) \frac{\partial u(s)}{\partial n_s} dB(s), \quad x \in D^c, \quad (2-10)$$

$$0 = \int_B M(s, x)u(s)dB(s) - \int_B L(s, x) \frac{\partial u(s)}{\partial n_s} dB(s), x \in D^c, \quad (2-11)$$

where D^c denotes the complementary domain.

2.2.3 Dual null-field integral formulation — the present version

By introducing the degenerate kernels, the collocation points can be located on the real boundary without facing the principal value. Therefore, the representations of integral equations including the boundary point can be written as

$$4\pi u(x) = \int_B T^I(s, x)u(s)dB(s) - \int_B U^I(s, x) \frac{\partial u(s)}{\partial n_s} dB(s), x \in D \cup B, \quad (2-12)$$

$$4\pi \frac{\partial u(x)}{\partial n_x} = \int_B M^I(s, x)u(s)dB(s) - \int_B L^I(s, x) \frac{\partial u(s)}{\partial n_s} dB(s), x \in D \cup B, \quad (2-13)$$

and

$$0 = \int_B T^E(s, x)u(s)dB(s) - \int_B U^E(s, x) \frac{\partial u(s)}{\partial n_s} dB(s), x \in D^c \cup B, \quad (2-14)$$

$$0 = \int_B M^E(s, x)u(s)dB(s) - \int_B L^E(s, x) \frac{\partial u(s)}{\partial n_s} dB(s), x \in D^c \cup B, \quad (2-15)$$

once the kernel is expressed in terms of an appropriate degenerate form. It is found that the collocation point is categorized to three positions, domain (Eqs.(2-2)-(2-3)), boundary (Eqs.(2-8)-(2-9)) and complementary domain (Eqs.(2-10)-(2-11)) in the conventional formulation. After using the degenerate kernel for the null-field BIEM, both Eqs.(2-12)-(2-13) and Eqs.(2-14)-(2-15) can contain the boundary point. The resulted linear algebraic systems derived from Eqs. (2-12)-(2-13) and Eqs. (2-14)-(2-15) are the same (Chen et al., 2006(a)), i.e. we can move to the boundary either from the domain point or null-field point.

2.2.4 Expansions of the fundamental solution and boundary density

The fundamental solution as previously mentioned is

$$U(s, x) = -\frac{e^{-ikr}}{r}, \quad (2-16)$$

where $r \equiv |s - x|$ is the distance between the source point and the field point and i is the imaginary number with $i^2 = -1$. To fully utilize the property of spherical geometry, the mathematical tools, degenerate (separable or finite rank) kernel and spherical harmonics, are utilized for the analytical calculation of boundary integrals.

2.2.4.1 Degenerate (separable) kernel for fundamental solutions

In the spherical coordinate, the field point (x) and source point (s) can be expressed as $x = (\rho, \phi, \theta)$ and $s = (\bar{\rho}, \bar{\phi}, \bar{\theta})$ in the spherical coordinate, respectively. By employing the addition theorem for separating the source point and field point, the kernel functions, $U(s, x)$, $T(s, x)$, $L(s, x)$ and $M(s, x)$, are expanded in terms of degenerate kernel as shown below:

$$U(s, x) = \begin{cases} U^I(s, x) = ik \sum_{n=0}^{\infty} (2n+1) \sum_{m=0}^n \varepsilon_m \frac{(n-m)!}{(n+m)!} \cos(m(\phi - \bar{\phi})) \\ \quad P_n^m(\cos \theta) P_n^m(\cos \bar{\theta}) j_n(k\rho) h_n^{(2)}(k\bar{\rho}), \bar{\rho} \geq \rho, \\ U^E(s, x) = ik \sum_{n=0}^{\infty} (2n+1) \sum_{m=0}^n \varepsilon_m \frac{(n-m)!}{(n+m)!} \cos(m(\phi - \bar{\phi})) \\ \quad P_n^m(\cos \theta) P_n^m(\cos \bar{\theta}) j_n(k\bar{\rho}) h_n^{(2)}(k\rho), \rho > \bar{\rho}. \end{cases} \quad (2-17)$$

$$T(s, x) = \begin{cases} T^I(s, x) = ik^2 \sum_{n=0}^{\infty} (2n+1) \sum_{m=0}^n \varepsilon_m \frac{(n-m)!}{(n+m)!} \cos(m(\phi - \bar{\phi})) \\ \quad P_n^m(\cos \theta) P_n^m(\cos \bar{\theta}) j_n(k\rho) h_n^{(2)}(k\bar{\rho}), \bar{\rho} > \rho, \\ T^E(s, x) = ik^2 \sum_{n=0}^{\infty} (2n+1) \sum_{m=0}^n \varepsilon_m \frac{(n-m)!}{(n+m)!} \cos(m(\phi - \bar{\phi})) \\ \quad P_n^m(\cos \theta) P_n^m(\cos \bar{\theta}) j'_n(k\bar{\rho}) h_n^{(2)}(k\rho), \rho > \bar{\rho}. \end{cases} \quad (2-18)$$

$$L(s, x) = \begin{cases} L^I(s, x) = ik^2 \sum_{n=0}^{\infty} (2n+1) \sum_{m=0}^n \varepsilon_m \frac{(n-m)!}{(n+m)!} \cos(m(\phi - \bar{\phi})) \\ \quad P_n^m(\cos \theta) P_n^m(\cos \bar{\theta}) j'_n(k\rho) h_n^{(2)}(k\bar{\rho}), \bar{\rho} > \rho, \\ L^E(s, x) = ik^2 \sum_{n=0}^{\infty} (2n+1) \sum_{m=0}^n \varepsilon_m \frac{(n-m)!}{(n+m)!} \cos(m(\phi - \bar{\phi})) \\ \quad P_n^m(\cos \theta) P_n^m(\cos \bar{\theta}) j_n(k\bar{\rho}) h_n^{(2)}(k\rho), \rho > \bar{\rho}. \end{cases} \quad (2-19)$$

$$M(s, x) = \begin{cases} M^I(s, x) = ik^3 \sum_{n=0}^{\infty} (2n+1) \sum_{m=0}^n \varepsilon_m \frac{(n-m)!}{(n+m)!} \cos(m(\phi - \bar{\phi})) \\ \quad P_n^m(\cos \theta) P_n^m(\cos \bar{\theta}) j'_n(k\rho) h_n^{(2)}(k\bar{\rho}), \bar{\rho} \geq \rho, \\ M^E(s, x) = ik^3 \sum_{n=0}^{\infty} (2n+1) \sum_{m=0}^n \varepsilon_m \frac{(n-m)!}{(n+m)!} \cos(m(\phi - \bar{\phi})) \\ \quad P_n^m(\cos \theta) P_n^m(\cos \bar{\theta}) j'_n(k\bar{\rho}) h_n^{(2)}(k\rho), \rho > \bar{\rho}. \end{cases} \quad (2-20)$$

where the superscripts “I” and “E” denote the interior and exterior regions, j_n and $h_n^{(2)}$ are the n th order spherical Bessel function of the first kind and the n th order spherical Hankel function of the second kind, respectively, P_n^m is the associated

Lengendre polynomial and ε_m is the Neumann factor,

$$\varepsilon_m = \begin{cases} 1, & m = 0, \\ 2, & m = 1, 2, \dots, \infty. \end{cases} \quad (2-21)$$

It is noted that U and M kernels in Eqs. (2-17) and (2-20) contain the equal sign of $\rho = \bar{\rho}$ while T and L kernels do not include the equal sign due to discontinuity in Eqs. (2-18) and (2-19). Besides, the potential across the boundary is also addressed here. For 2-D Laplace and Helmholtz equations, the continuous and jump behavior across the boundary were studied respectively in (Chen and Chen, 2007) and (Chen et al., 2007). After using the Wronskian property of $j_m(\cdot)$ and $y_m(\cdot)$, we have

$$W(j_m(k\rho), y_m(k\rho)) = j_m(k\rho)y'_m(k\rho) - j'_m(k\rho)y_m(k\rho) = \frac{1}{k\rho^2}. \quad (2-22)$$

The jump behavior is well captured by

$$\begin{aligned} \int_0^{2\pi} \int_0^\pi [T^I(s, x) - T^E(s, x)] P_n^m(\cos\bar{\theta}) \cos(m\bar{\phi}) R^2 \sin(m\bar{\theta}) d\bar{\theta} d\bar{\phi} \\ = P_n^m(\cos\theta) \cos(m\phi) \end{aligned} \quad (2-23)$$

Similarly, the potentials due to L^I and L^E kernels are discontinuous across the boundary.

2.2.4.2 Spherical harmonics for boundary densities

We used the spherical harmonics to approximate the boundary density and its normal derivative as expressed by

$$u(s) = \sum_{v=0}^{\infty} \sum_{w=0}^v A_{vw} P_v^w(\cos\bar{\theta}) \cos(w\bar{\phi}), \quad s \in B, \quad (2-24)$$

$$t(s) = \frac{\partial u(s)}{\partial n_s} = \sum_{v=0}^{\infty} \sum_{w=0}^v B_{vw} P_v^w(\cos\bar{\theta}) \cos(w\bar{\phi}), \quad s \in B, \quad (2-25)$$

where A_{vw} and B_{vw} are the unknown coefficients.

2.3 Proof of the existence of spurious eigensolutions for a concentric sphere

In order to fully utilize the geometry of spherical boundary, the potential u and its normal derivative t can be approximated by employing the spherical harmonic functions. Therefore, the following expressions can be obtained

$$u_1(s) = \sum_{v=0}^{\infty} \sum_{w=0}^v A_{vw}^1 P_v^w(\cos\bar{\theta}) \cos(w\bar{\phi}), \quad s \in B_1, \quad (2-26)$$

$$u_2(s) = \sum_{v=0}^{\infty} \sum_{w=0}^v A_{vw}^2 P_v^w(\cos \bar{\theta}) \cos(w\bar{\phi}), \quad s \in B_2, \quad (2-27)$$

$$t_1(s) = \sum_{v=0}^{\infty} \sum_{w=0}^v B_{vw}^1 P_v^w(\cos \bar{\theta}) \cos(w\bar{\phi}), \quad s \in B_1, \quad (2-28)$$

$$t_2(s) = \sum_{v=0}^{\infty} \sum_{w=0}^v B_{vw}^2 P_v^w(\cos \bar{\theta}) \cos(w\bar{\phi}), \quad s \in B_2, \quad (2-29)$$

where A_{vw}^i and B_{vw}^i are the spherical coefficients on B_i ($i=1,2$). When the field point is located on the inner boundary B_1 , substitution of Eqs. (2-26)-(2-29) into the null-field integral equations yields

$$\begin{aligned} 0 = & \int_0^{2\pi} \int_0^{\pi} \sum_{n=0}^{\infty} \sum_{m=0}^n \sum_{v=0}^{\infty} \sum_{w=0}^v ik^2 \varepsilon_m A_{vw}^1 (2n+1) \frac{(n-m)!}{(n+m)!} j_n(k\rho) h_n^{(2)}(kR_1) P_n^m(\cos(\theta)) \cdot \\ & \cos(m(\phi - \bar{\phi})) \cos(w\bar{\phi}) P_n^m(\cos(\bar{\theta})) P_v^w(\cos(\bar{\theta})) \sin(\bar{\theta}) R_1^2 d\bar{\theta} d\bar{\phi} \\ & - \int_0^{2\pi} \int_0^{\pi} \sum_{n=0}^{\infty} \sum_{m=0}^n \sum_{v=0}^{\infty} \sum_{w=0}^v ik \varepsilon_m B_{vw}^1 (2n+1) \frac{(n-m)!}{(n+m)!} j_n(k\rho) h_n^{(2)}(kR_1) P_n^m(\cos(\theta)) \cdot \\ & \cos(m(\phi - \bar{\phi})) \cos(w\bar{\phi}) P_n^m(\cos(\bar{\theta})) P_v^w(\cos(\bar{\theta})) \sin(\bar{\theta}) R_1^2 d\bar{\theta} d\bar{\phi} \\ & + \int_0^{2\pi} \int_0^{\pi} \sum_{n=0}^{\infty} \sum_{m=0}^n \sum_{v=0}^{\infty} \sum_{w=0}^v ik^2 \varepsilon_m A_{vw}^2 (2n+1) \frac{(n-m)!}{(n+m)!} j_n(k\rho) h_n^{(2)}(kR_2) P_n^m(\cos(\theta)) \cdot \\ & \cos(m(\phi - \bar{\phi})) \cos(w\bar{\phi}) P_n^m(\cos(\bar{\theta})) P_v^w(\cos(\bar{\theta})) \sin(\bar{\theta}) R_2^2 d\bar{\theta} d\bar{\phi} \\ & - \int_0^{2\pi} \int_0^{\pi} \sum_{n=0}^{\infty} \sum_{m=0}^n \sum_{v=0}^{\infty} \sum_{w=0}^v ik \varepsilon_m B_{vw}^2 (2n+1) \frac{(n-m)!}{(n+m)!} j_n(k\rho) h_n^{(2)}(kR_2) P_n^m(\cos(\theta)) \cdot \\ & \cos(m(\phi - \bar{\phi})) \cos(w\bar{\phi}) P_n^m(\cos(\bar{\theta})) P_v^w(\cos(\bar{\theta})) \sin(\bar{\theta}) R_2^2 d\bar{\theta} d\bar{\phi}. \end{aligned} \quad (2-30)$$

When the field point is located on the outer boundary B_2 , we have

$$\begin{aligned} 0 = & \int_0^{2\pi} \int_0^{\pi} \sum_{n=0}^{\infty} \sum_{m=0}^n \sum_{v=0}^{\infty} \sum_{w=0}^v ik^2 \varepsilon_m A_{vw}^1 (2n+1) \frac{(n-m)!}{(n+m)!} j'_n(kR_1) h_n^{(2)}(k\rho) P_n^m(\cos(\theta)) \cdot \\ & \cos(m(\phi - \bar{\phi})) \cos(w\bar{\phi}) P_n^m(\cos(\bar{\theta})) P_v^w(\cos(\bar{\theta})) \sin(\bar{\theta}) R_1^2 d\bar{\theta} d\bar{\phi} \\ & - \int_0^{2\pi} \int_0^{\pi} \sum_{n=0}^{\infty} \sum_{m=0}^n \sum_{v=0}^{\infty} \sum_{w=0}^v ik \varepsilon_m B_{vw}^1 (2n+1) \frac{(n-m)!}{(n+m)!} j_n(kR_1) h_n^{(2)}(k\rho) P_n^m(\cos(\theta)) \cdot \\ & \cos(m(\phi - \bar{\phi})) \cos(w\bar{\phi}) P_n^m(\cos(\bar{\theta})) P_v^w(\cos(\bar{\theta})) \sin(\bar{\theta}) R_1^2 d\bar{\theta} d\bar{\phi} \\ & + \int_0^{2\pi} \int_0^{\pi} \sum_{n=0}^{\infty} \sum_{m=0}^n \sum_{v=0}^{\infty} \sum_{w=0}^v ik^2 \varepsilon_m A_{vw}^2 (2n+1) \frac{(n-m)!}{(n+m)!} j'_n(kR_2) h_n^{(2)}(k\rho) P_n^m(\cos(\theta)) \cdot \\ & \cos(m(\phi - \bar{\phi})) \cos(w\bar{\phi}) P_n^m(\cos(\bar{\theta})) P_v^w(\cos(\bar{\theta})) \sin(\bar{\theta}) R_2^2 d\bar{\theta} d\bar{\phi} \\ & - \int_0^{2\pi} \int_0^{\pi} \sum_{n=0}^{\infty} \sum_{m=0}^n \sum_{v=0}^{\infty} \sum_{w=0}^v ik \varepsilon_m B_{vw}^2 (2n+1) \frac{(n-m)!}{(n+m)!} j_n(kR_2) h_n^{(2)}(k\rho) P_n^m(\cos(\theta)) \cdot \\ & \cos(m(\phi - \bar{\phi})) \cos(w\bar{\phi}) P_n^m(\cos(\bar{\theta})) P_v^w(\cos(\bar{\theta})) \sin(\bar{\theta}) R_2^2 d\bar{\theta} d\bar{\phi}. \end{aligned} \quad (2-31)$$

For the Dirichlet problem, Eqs. (2-30) and (2-31) can be reduced to

$$0 = \sum_{n=0}^{\infty} \sum_{m=0}^n a^2 k B_{nm}^1 j_n(ka) h_n^{(2)}(ka) P_n^m(\cos(\theta)) \cos(m\phi) + \sum_{n=0}^{\infty} \sum_{m=0}^n b^2 k B_{nm}^2 j_n(kb) h_n^{(2)}(kb) P_n^m(\cos(\theta)) \cos(m\phi), \quad (2-32)$$

$$0 = \sum_{n=0}^{\infty} \sum_{m=0}^n a^2 k B_{nm}^1 j_n(ka) h_n^{(2)}(kb) P_n^m(\cos(\theta)) \cos(m\phi) + \sum_{n=0}^{\infty} \sum_{m=0}^n b^2 k B_{nm}^2 j_n(kb) h_n^{(2)}(kb) P_n^m(\cos(\theta)) \cos(m\phi). \quad (2-33)$$

According to Eqs. (2-32) and (2-33), the spherical coefficients B_{nm}^1 and B_{nm}^2 satisfy the relations:

$$B_{nm}^2 = -\frac{a^2 j_n(ka) h_n^{(2)}(ka)}{b^2 j_n(ka) h_n^{(2)}(kb)} B_{nm}^1, \quad (2-34)$$

$$B_{nm}^2 = -\frac{a^2 j_n(ka) h_n^{(2)}(kb)}{b^2 j_n(kb) h_n^{(2)}(kb)} B_{nm}^1. \quad (2-35)$$

To seek the nontrivial data for the spherical coefficients B_{nm}^1 and B_{nm}^2 , we obtain the eigenequation:

$$j_n(ka) h_n^{(2)}(kb) \left[j_n(kb) h_n^{(2)}(ka) - j_n(ka) h_n^{(2)}(kb) \right] = 0 \quad (2-36)$$

For the Neumann problem, Eqs. (2-30) and (2-31) are reduced to

$$0 = \sum_{n=0}^{\infty} \sum_{m=0}^n a^2 A_{nm}^1 j_n(ka) h_n'^{(2)}(ka) + \sum_{n=0}^{\infty} \sum_{m=0}^n b^2 A_{nm}^2 j_n(ka) h_n'^{(2)}(kb), \quad (2-37)$$

$$0 = \sum_{n=0}^{\infty} \sum_{m=0}^n a^2 A_{nm}^1 j_n(ka) h_n'^{(2)}(kb) + \sum_{n=0}^{\infty} \sum_{m=0}^n b^2 A_{nm}^2 j_n(kb) h_n'^{(2)}(kb). \quad (2-38)$$

According to Eqs. (2-37) and (2-38), the spherical coefficients A_{nm}^1 and A_{nm}^2 satisfy the relations:

$$A_{nm}^2 = -\frac{a^2 j_n(ka) h_n'^{(2)}(ka)}{b^2 j_n(ka) h_n'^{(2)}(kb)} A_{nm}^1, \quad (2-39)$$

$$A_{nm}^2 = -\frac{a^2 j_n'(ka) h_n^{(2)}(kb)}{b^2 j_n'(kb) h_n^{(2)}(kb)} A_{nm}^1. \quad (2-40)$$

To seek the nontrivial data for the spherical coefficients A_{nm}^1 and A_{nm}^2 , we obtain the eigenequation:

$$j_n(ka) h_n^{(2)}(kb) \left[j_n'(kb) h_n'^{(2)}(ka) - j_n'(ka) h_n'^{(2)}(kb) \right] = 0. \quad (2-41)$$

According to Eqs. (2-36) and (2-41), the spurious eigenequation of the singular formulation is $j_n(ka) = 0$, which is also the true eigenequation of the sphere of radius a with the fixed boundary condition. The latter parts in the bracket of Eqs. (2-36) and (2-41) are the true eigenequations,

$$j_n(kb) h_n^{(2)}(ka) - j_n(ka) h_n^{(2)}(kb) = 0 \quad \text{for the Dirichlet problem} \quad (2-42)$$

$$j'_n(kb)h_n^{(2)}(ka) - j'_n(ka)h_n^{(2)}(kb) = 0 \quad \text{for the Neumann problem} \quad (2-43)$$

The spurious and true eigenequations of the concentric sphere subject to various boundary conditions are listed in Table 2-1. It is interesting to find that spurious eigenvalue of *UT* singular method results in trivial outer boundary modes for the fixed-fixed case. Besides, spurious eigenvalue of *LM* hypersingular method results in the trivial outer boundary modes of free-free case.

2.4 Proof the existence for the spurious eigensolutions of the concentric sphere

In order to prove that the spurious eigensolutions is the true eigenvalue of the associated problem bounded by inner boundary, we first derive the true eigenvalue of the eigenproblem bounded by the inner boundary. Now, we consider the sphere with a radius a in the continuous system. By using the null-field integral equation and collocating the point on the boundary, we obtain the true eigenequation

$$j_n(ka) = 0, \quad (2-44)$$

and the corresponding true eigenmode is B_{nm} , where $\sum \sum |B_{nm}| \neq 0$. By collocating the point in the complementary domain ($x^c \in D^c$) as shown in Fig. 2-2, the null-field equation yields

$$0 = \int_{B_1} U^E(s, x^c) t(s) dB(s), \quad x^c \in D^c. \quad (2-45)$$

We can obtain the null-field response for x^c as shown below

$$B_{nm}^1 j_n(ka) h_n^{(2)}(ka^+) P_n^m(\cos(\theta)) \cos(m\phi) = 0, \quad (2-46)$$

where n and m belong to nature number and k satisfies Eq. (2-44). Secondly, we consider the spherical case with the fixed-fixed boundary condition as shown in Fig. 2-3. By selecting a nontrivial inner boundary mode for the boundary mode and trivial outer boundary mode, we have $j_n(ka) = 0$ and

$$\begin{cases} B_{nm}^1 \\ B_{nm}^2 \end{cases} = \begin{cases} B_{nm} \\ 0 \end{cases} \quad (2-47)$$

This indicates that spurious eigenevalues of $j_n(ka) = 0$ and the nontrivial boundary mode of Eq. (2-47) satisfy Eqs. (2-32) and (2-33) due to $U^I(s, a^-) = U^E(x, a^+)$. Therefore, spurious eigenvalues in conjunction with the trivial outer boundary mode happen to be the true eigenvalue of the domain bounded by the inner boundary. Similarly, the concentric sphere subjected to the Neumann boundary condition by using

the hypersingular formulation results in the trivial outer boundary mode.

2.5 SVD technique for extracting out true and spurious eigenvalues by using updating terms and updating documents

2.5.1 Method of extracting the true eigensolutions (updating terms)

SVD technique is an important tool in the linear algebra. The matrix $[\mathbf{A}]$ with a dimension M by N can be decomposed into a product of the unitary matrix $[\Phi]$ (M by M), the matrix $[\Sigma]$ (M by N) with positive or zero elements, and the unitary matrix $[\Psi]$ (N by N)

$$[\mathbf{A}]_{M \times N} = [\Phi]_{M \times M} [\Sigma]_{M \times N} [\Psi]_{N \times N}^H, \quad (2-48)$$

where the superscript “ H ” is the Hermitian operator, $[\Phi]$ and $[\Psi]$ are both unitary matrix that their column vectors which satisfy

$$\phi_i^H \cdot \phi_j = \delta_{ij}, \quad (2-49)$$

$$\psi_i^H \cdot \psi_j = \delta_{ij}, \quad (2-50)$$

in which $[\Phi]^H [\Phi] = [\mathbf{I}]_{M \times M}$ and $[\Psi]^H [\Psi] = [\mathbf{I}]_{N \times N}$. For the eigenproblem, we can obtain a nontrivial solution for the homogeneous system from a column vector $\{\psi_i\}$ of $[\Psi]$ when the corresponding singular value (σ_i) is zero. For the direct BEM, we have

Singular formulation (UT method)

$$[\mathbf{T}^E] \{u\} = [\mathbf{U}^E] \{t\} = \{0\}, \quad (2-51)$$

Hypersingular formulation (LM method)

$$[\mathbf{M}^E] \{u\} = [\mathbf{L}^E] \{t\} = \{0\}, \quad (2-52)$$

where $\{u\}$ and $\{t\}$ are the boundary densities. For the Dirichlet problem, Eq. (2-51) and (2-52) can be combined to have

$$\begin{bmatrix} \mathbf{U}^E \\ \mathbf{L}^E \end{bmatrix} \{t\} = \{0\}. \quad (2-53)$$

By using the SVD technique, the two submatrices in Eqs. (2-51) and (2-52) can be decomposed into

$$[\mathbf{U}^E] = [\Phi^{(U)}] [\Sigma^{(U)}] [\Psi^{(U)}]^H \quad \text{or} \quad [\mathbf{U}^E] = \sum_j \sigma_j^{(U)} \{\phi_j^{(U)}\} \{\psi_j^{(U)}\}^H, \quad (2-54)$$

$$[\mathbf{L}^E] = [\Phi^{(L)}] [\Sigma^{(L)}] [\Psi^{(L)}]^H \quad \text{or} \quad [\mathbf{L}^E] = \sum_j \sigma_j^{(L)} \{\phi_j^{(L)}\} \{\psi_j^{(L)}\}^H. \quad (2-55)$$

where the superscripts, (U) and (L) , denote the corresponding matrices. For the linear

algebraic system, $\{t\}$ is a column vector of $\{\psi_i\}$ in the matrix $[\Psi]$ corresponding to the zero singular value ($\sigma_i = 0$). By setting $\{t\}$ as a vector of $\{\psi_i\}$ in the right unitary matrix for the true eigenvalue k_i , Eqs. (2-51) and (2-52) reduces to

$$[\mathbf{U}^E(k_i)]\{\psi_i\} = \{0\}, \quad (2-56)$$

$$[\mathbf{L}^E(k_i)]\{\psi_i\} = \{0\}. \quad (2-57)$$

According to Eqs. (2-54) and (2-55), we have

$$\sigma_j^{(U)}\{\phi_j^{(U)}\} = \{0\}, \quad (2-58)$$

$$\sigma_j^{(L)}\{\phi_j^{(L)}\} = \{0\}. \quad (2-59)$$

We can easily extract out the true eigenvalues, $\sigma_j^{(U)} = \sigma_j^{(L)} = \{0\}$, since there exists the same eigensolution ($\{t\} = \{\psi_i\}$) for the Dirichlet problem by using Eqs. (2-53) or (2-56) and (2-58). In a similar way, Eqs. (2-51) and (2-52) can be combined to have

$$\begin{bmatrix} \mathbf{T}^E(k_i) \\ \mathbf{M}^E(k_i) \end{bmatrix} \{u\} = \{0\}, \quad (2-60)$$

for the Neumann problem. We can easily extract out the true eigenvalues for the Neumann problem with respect to the j th zero singular values of $\sigma_j^{(T)} = \sigma_j^{(M)} = \{0\}$.

2.5.2 Method of filtering out the spurious eigensolutions (updating documents)

By employing the LM formulation in the direct BEM, we have

$$[\mathbf{M}^E]\{u\} = [\mathbf{L}^E]\{t\} = \{p\}. \quad (2-61)$$

Since the spurious eigenvalue k_s is embedded in both the Dirichlet and Neumann problems, we have

$$\{p\}^H \{\phi_i\} = \{0\}, \quad (2-62)$$

where $\{\phi_i\}$ satisfies

$$[\mathbf{L}^E(k_s)]^H \{\phi_i\} = \{0\} \quad \text{for the Dirichlet problem,} \quad (2-63)$$

$$[\mathbf{M}^E(k_s)]^H \{\phi_i\} = \{0\} \quad \text{for the Neumann problem,} \quad (2-64)$$

according to the Fredholm alternative theorem. By substituting Eq. (2-61) into Eqs. (2-62), (2-63) and (2-64), we have

$$\{u\}^H [\mathbf{M}^E(k_s)]^H \{\phi_i\} = \{0\} \quad \text{for the Dirichlet problem,} \quad (2-65)$$

$$\{t\}^H [\mathbf{L}^E(k_s)]^H \{\phi_i\} = \{0\} \quad \text{for the Neumann problem.} \quad (2-66)$$

Since $\{u\}$ and $\{t\}$ can be arbitrary boundary excitation for the Dirichlet problem and

Neumann problem, respectively, this yields

$$\left[\mathbf{M}^E(k_s) \right]^H \{ \phi_i \} = \{ 0 \} \quad \text{for the Dirichlet problem} \quad (2-67)$$

$$\left[\mathbf{L}^E(k_s) \right]^H \{ \phi_i \} = \{ 0 \} \quad \text{for the Neumann problem} \quad (2-68)$$

By combining Eq. (2-63) with Eq. (2-67) for the Dirichlet problem, we have

$$\begin{bmatrix} \left[\mathbf{L}^E \right]^H \\ \left[\mathbf{M}^E \right]^H \end{bmatrix} \{ \phi_i \} = \{ 0 \} \quad \text{or} \quad \{ \phi_i \}^H \begin{bmatrix} \left[\mathbf{L}^E \right] \\ \left[\mathbf{M}^E \right] \end{bmatrix} = \{ 0 \}. \quad (2-69)$$

It indicates that two matrices have the same spurious boundary mode $\{ \phi_i \}$ corresponding to the i th zero singular values. By using the SVD technique, two matrices in Eq. (2-69) can be decomposed into

$$\left[\mathbf{L}^E \right]^H = \left[\Psi^{(L)} \right] \left[\Sigma^{(L)} \right] \left[\Phi^{(L)} \right]^H \quad \text{or} \quad \left[\mathbf{L}^E \right] = \sum_j \sigma_j^{(L)} \{ \psi_j^{(L)} \} \{ \phi_j^{(L)} \}^H, \quad (2-70)$$

$$\left[\mathbf{M}^E \right]^H = \left[\Psi^{(M)} \right] \left[\Sigma^{(M)} \right] \left[\Phi^{(M)} \right]^H \quad \text{or} \quad \left[\mathbf{M}^E \right] = \sum_j \sigma_j^{(M)} \{ \psi_j^{(M)} \} \{ \phi_j^{(M)} \}^H. \quad (2-71)$$

By substituting Eqs. (2-70) and (2-71) into Eqs. (2-65) and (2-66), we have

$$\sigma_j^{(L)} \{ \psi_j^{(L)} \} = \{ 0 \}, \quad (2-72)$$

$$\sigma_j^{(M)} \{ \psi_j^{(M)} \} = \{ 0 \}. \quad (2-73)$$

We can easily extract out the spurious eigenvalues since there exists the same spurious boundary mode $\{ \phi_i \}$ corresponding the i th zero singular value, $\sigma_i^{(L)} = \sigma_i^{(M)} = 0$. Similarly, the spurious eigenvalue parasitized in the UT formulation can be obtained by using SVD updating documents. To summarize the SVD structure for the four influence matrices, Table 2-2 (a) and (b) show that the spurious and true boundary modes are imbedded in the left and right unitary vectors, respectively. Besides, the nontrivial interior boundary mode and trivial outer boundary mode are also given in Table 2-2 (b).

2.6 Illustrative examples and discussions

Case 1: A concentric sphere subject to the Dirichlet boundary condition ($u_1 = u_2 = 0$)

A concentric case with radii a and b ($a = 0.5$ and $b = 1.0$) is shown in Fig. 2-1.

The analytical solution can be obtained by using the null-filled integral formulation, degenerate kernel and spherical harmonics. The common drop locations in Figs. 2-4(a)

and 2-4(b) indicate the true eigenvalues. We employ the SVD updating term $\begin{bmatrix} U \\ L \end{bmatrix}$ to

extract the true eigenvalues for the Dirichlet problem as shown in Fig. 2-4(c). It's found that all the spurious eigenvalues are filtered out.

Case 2: A concentric sphere subject to the Neumann boundary condition ($t_1 = t_2 = 0$)

Similarly, the common drop locations in Figs. 2-4(d) and 2-4(e) indicate the true eigenvalues. Extraction of true eigenvalues by using the SVD updating term $\begin{bmatrix} T \\ M \end{bmatrix}$ is shown in Fig. 2-4(f). The common drop locations in Figs. 2-5(a) and 2-5(b) indicate the spurious eigenvalues for the singular formulation. Similarly, the same drop locations in Figs. 2-5(d) and 2-5(e) indicate the spurious eigenvalues for the hypersingular formulation. The spurious eigenequations for the singular and hypersingular formulation are

$$j_n(ka) = 0, \quad (2-74)$$

$$j'_n(ka) = 0, \quad (2-75)$$

respectively. It's found that spurious eigenvalues depend on the inner boundary instead of the outer boundary. Finally, we employed the SVD updating document to filter out the spurious eigenvalues. The spurious eigenvalues for singular formulation and hypersingular formulation are extracted as shown in Figs. 2-5(c) and 2-5(f), respectively.

2.7 Conclusions

Spurious eigenvalues for a concentric sphere were studied analytically and numerically. One example was demonstrated to see how the spurious eigenvalues occur in the concentric sphere. Spurious eigenvalues depend on the inner boundary and are independent of the outer boundary. The trivial outer boundary densities were examined in case of the spurious eigenvalue which is found to be the true eigenvalue for the domain bounded by the inner boundary. The contribution of the work is to show the existence of spurious eigenvalue for a concentric sphere in an analytical manner by using the degenerate kernels and the spherical harmonics.

Table 2-1 Eigensolutions and boundary modes for the concentric sphere subject to different boundary conditions

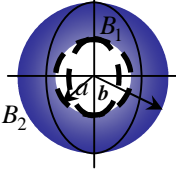
	BC	Fixed-fixed $u_1 = u_2 = 0$	Free-fixed $t_1 = u_2 = 0$	Fixed-free $u_1 = t_2 = 0$	Free-free $t_1 = t_2 = 0$
	Solution				
UT formulation	True eigenequation	$j_n(ka)y_n(kb)$ $-j_n(kb)y_n(ka) = 0$	$j'_n(ka)y_n(kb)$ $-j_n(kb)y'_n(ka) = 0$	$j_n(ka)y'_n(kb)$ $-j'_n(kb)y_n(ka) = 0$	$j'_n(ka)y'_n(kb)$ $-j'_n(kb)y'_n(ka) = 0$
	Spurious eigenequation	$j_n(ka) = 0$	$j_n(ka) = 0$	$j_n(ka) = 0$	$j_n(ka) = 0$
	Inner boundary mode	$\sum \sum B_{nm} \neq 0$	$\sum \sum A_{nm} \neq 0$	$\sum \sum B_{nm} \neq 0$	$\sum \sum A_{nm} \neq 0$
	Outer boundary mode	$B_{nm}^2 = \frac{a^2 j_n(ka)}{b^2 j_n(kb)} B_{nm}^1$	$B_{nm}^2 = \frac{a^2 j'_n(ka)}{b^2 j_n(kb)} A_{nm}^1$	$A_{nm}^2 = \frac{a^2 j_n(ka)}{b^2 j'_n(kb)} B_{nm}^1$	$A_{nm}^2 = \frac{a^2 j'_n(ka)}{b^2 j'_n(kb)} A_{nm}^1$
LM formulation	True eigenequation	$j_n(ka)y_n(kb)$ $-j_n(kb)y_n(ka) = 0$	$j'_n(ka)y_n(kb)$ $-j_n(kb)y'_n(ka) = 0$	$j_n(ka)y'_n(kb)$ $-j'_n(kb)y_n(ka) = 0$	$j'_n(ka)y'_n(kb)$ $-j'_n(kb)y'_n(ka) = 0$
	Spurious eigenequation	$j'_n(ka) = 0$	$j'_n(ka) = 0$	$j'_n(ka) = 0$	$j'_n(ka) = 0$
	Inner boundary mode	$\sum \sum B_{nm} \neq 0$	$\sum \sum A_{nm} \neq 0$	$\sum \sum B_{nm} \neq 0$	$\sum \sum A_{nm} \neq 0$
	Outer boundary mode	$B_{nm}^2 = \frac{a^2 j_n(ka)}{b^2 j_n(kb)} B_{nm}^1$	$B_{nm}^2 = \frac{a^2 j'_n(ka)}{b^2 j_n(kb)} A_{nm}^1$	$A_{nm}^2 = \frac{a^2 j_n(ka)}{b^2 j'_n(kb)} B_{nm}^1$	$A_{nm}^2 = \frac{a^2 j'_n(ka)}{b^2 j'_n(kb)} A_{nm}^1$

Table 2-2(a) SVD structure of the four influence matrices for the Dirichlet and Neumann problems in the case of true eigenvalue.

	Dirichlet problem ($k = k_T^D$)		Neumann problem ($k = k_T^N$)	
True eigenvalue k_T (k_T^D, k_T^N)	$[\Phi^U] \begin{bmatrix} 0 & & \\ & \ddots & \\ & & \varphi_{\tilde{1}}^D \cdots \end{bmatrix}^H$ <p>The same $\varphi_{\tilde{1}}^D$</p>	$[\Phi^T][\Sigma^T][\Psi^T]^H$	$[\Phi^U][\Sigma^U][\Psi^U]^H$	$[\Phi^T] \begin{bmatrix} 0 & & \\ & \ddots & \\ & & \varphi_{\tilde{1}}^N \cdots \end{bmatrix}^H$ <p>The same $\varphi_{\tilde{1}}^N$</p>
	$[\Phi^L] \begin{bmatrix} 0 & & \\ & \ddots & \\ & & \varphi_{\tilde{1}}^D \cdots \end{bmatrix}^H$	$[\Phi^M][\Sigma^M][\Psi^M]^H$	$[\Phi^L][\Sigma^L][\Psi^L]^H$	$[\Phi^M] \begin{bmatrix} 0 & & \\ & \ddots & \\ & & \varphi_{\tilde{1}}^N \cdots \end{bmatrix}^H$

where k_T^D and k_T^N denotes the true eigenvalues for the Dirichlet and Neumann problems, respectively.

Table 2-2(b) SVD structure of the four influence matrices by using the UT singular formulation and LM hypersingular formulation in the case of spurious eigenvalue.

	UT singular formulation ($k = k_s^{UT}$)		LM hypersingular formulation ($k = k_s^{LM}$)	
	Dirichlet	Neumann	Dirichlet	Neumann
Spurious eigenvalue k_s (k_s^{UT}, k_s^{LM})	$\begin{bmatrix} \phi_1^{UT} & \dots \\ \vdots & \vdots \end{bmatrix} \begin{bmatrix} 0 & & \\ & \ddots & \\ & & 0 \end{bmatrix} \begin{bmatrix} \phi_1^D & \dots \\ \vdots & \vdots \\ \{0\} & \dots \end{bmatrix}^H$	$\begin{bmatrix} \phi_1^{UT} & \dots \\ \vdots & \vdots \end{bmatrix} \begin{bmatrix} 0 & & \\ & \ddots & \\ & & 0 \end{bmatrix} \begin{bmatrix} \Psi^T \\ \vdots \\ \vdots \end{bmatrix}^H$	$\begin{bmatrix} \phi_1^{LM} & \dots \\ \vdots & \vdots \end{bmatrix} \begin{bmatrix} 0 & & \\ & \ddots & \\ & & 0 \end{bmatrix} \begin{bmatrix} \Psi^L \\ \vdots \\ \vdots \end{bmatrix}^H$	$\begin{bmatrix} \phi_1^{LM} & \dots \\ \vdots & \vdots \end{bmatrix} \begin{bmatrix} 0 & & \\ & \ddots & \\ & & 0 \end{bmatrix} \begin{bmatrix} \phi_1^N & \dots \\ \vdots & \vdots \\ \{0\} & \dots \end{bmatrix}^H$
	The same ϕ^{UT}		The same ϕ^{LM}	
	U	T	L	M

where k_s^{UT} and k_s^{LM} denotes the spurious eigenvalues by using UT singular and LM hypersingular formulation, respectively.

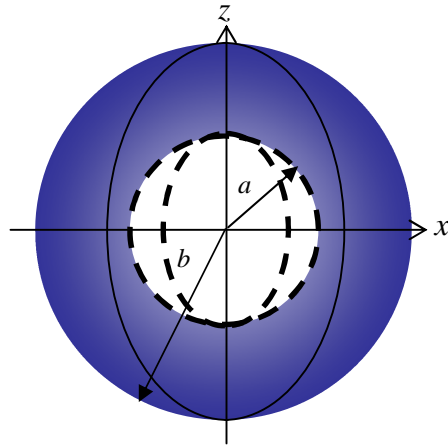


Figure 2-1 Sketch of a concentric sphere

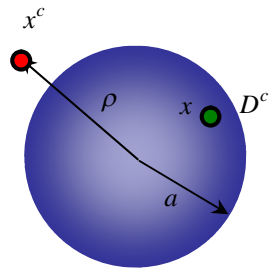


Figure 2-2 Collocation point on the sphere boundary from the null-field point ($\rho = a^+$)

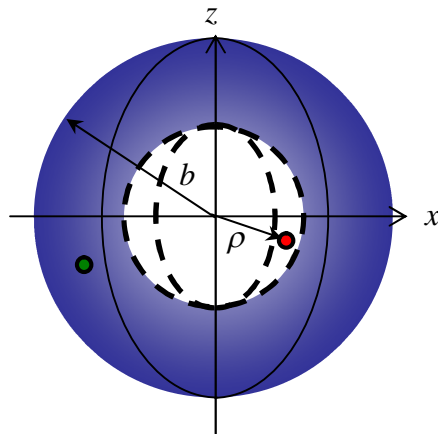
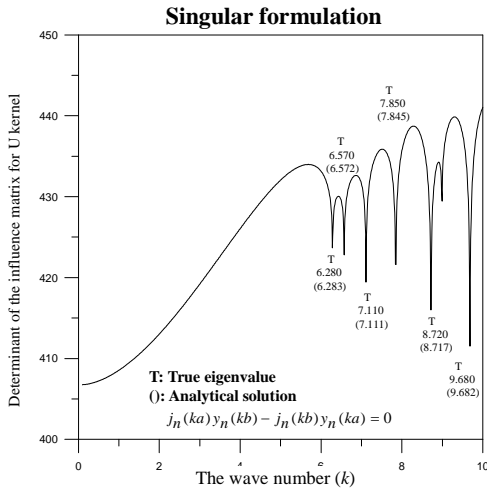
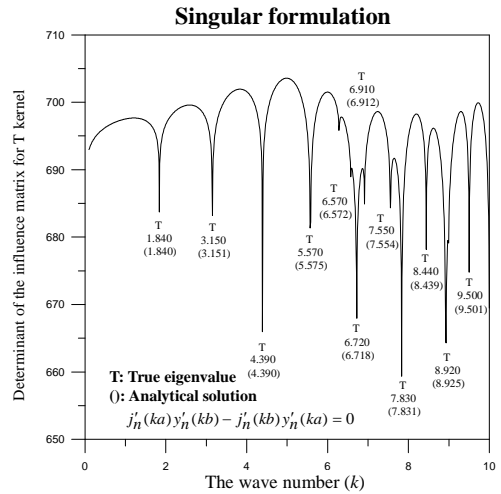


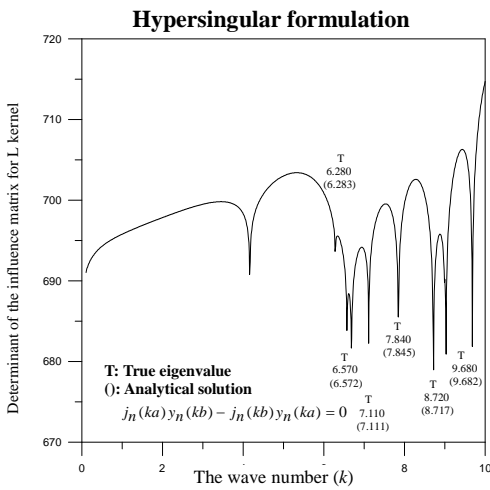
Figure 2-3 Collocation point of the concentric sphere ($\rho = a^-$)



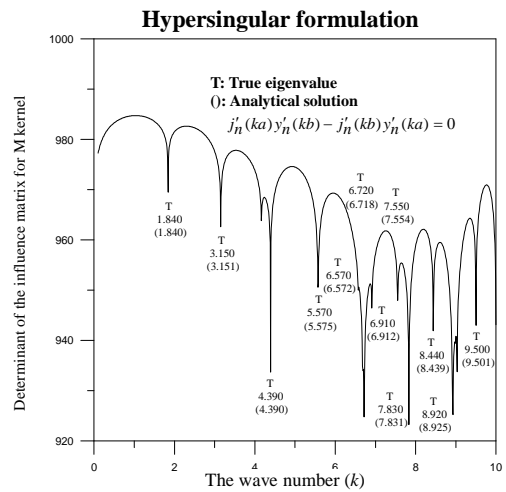
(a) Determinant versus the wave number by using the singular formulation for the Dirichlet condition.



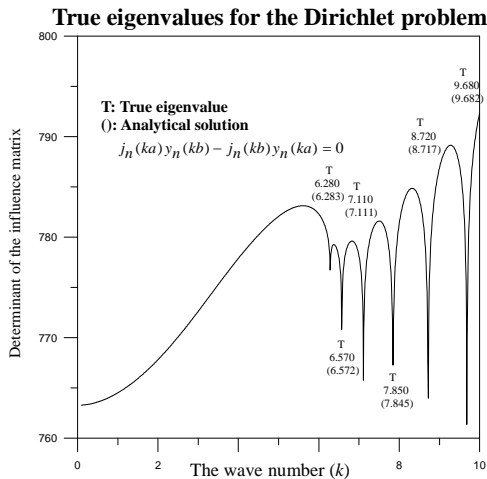
(d) Determinant versus the wave numbers by using the singular formulation for the Neumann condition.



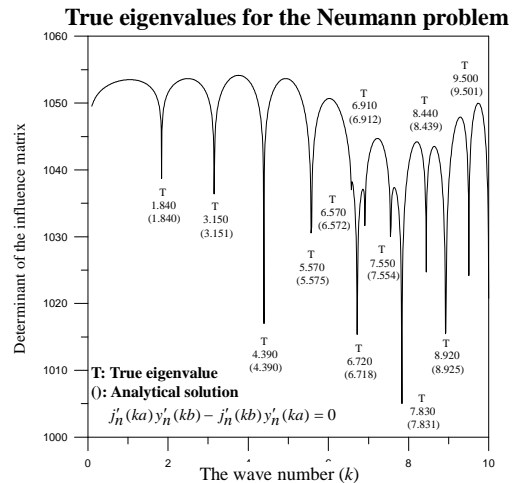
(b) Determinant versus the wave number by using the hypersingular formulation for the Dirichlet condition.



(e) Determinant versus the wave number by using the hypersingular formulation for the Neumann condition.

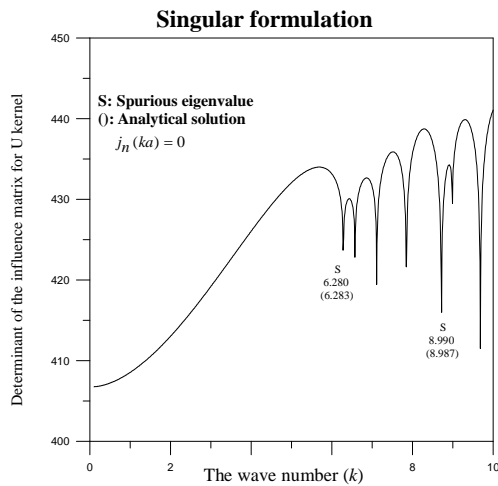


(c) Extraction of true eigenvalues for the Dirichlet problem by using the SVD updating terms.

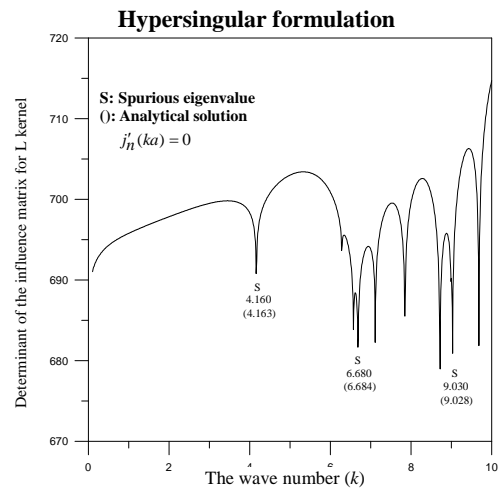


(f) Extraction of true eigenvalues for the Neumann problem by using the SVD updating terms.

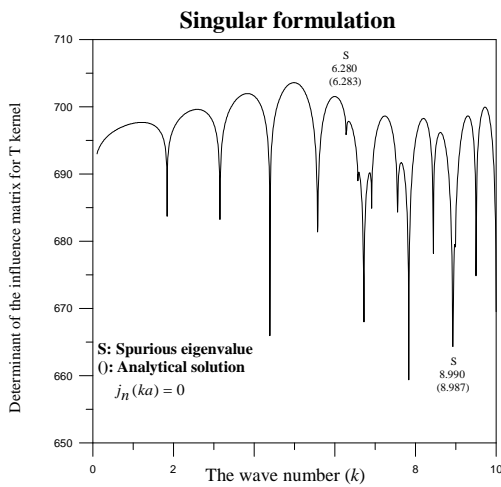
Figure 2-4 True eigenvalues for a concentric sphere by using the SVD updating terms ($a = 0.5$ and $b = 1.0$).



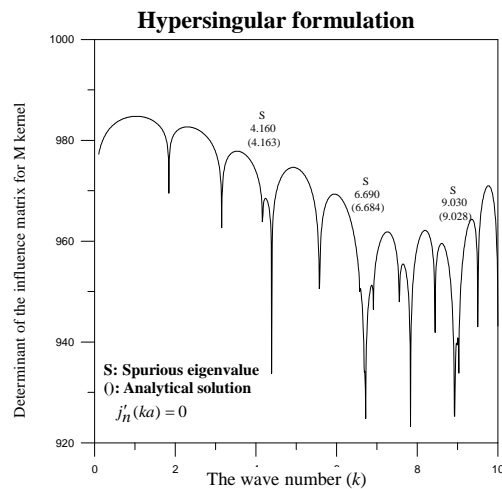
(a) Determinant versus the wave number by using the singular formulation subject to the Dirichlet condition.



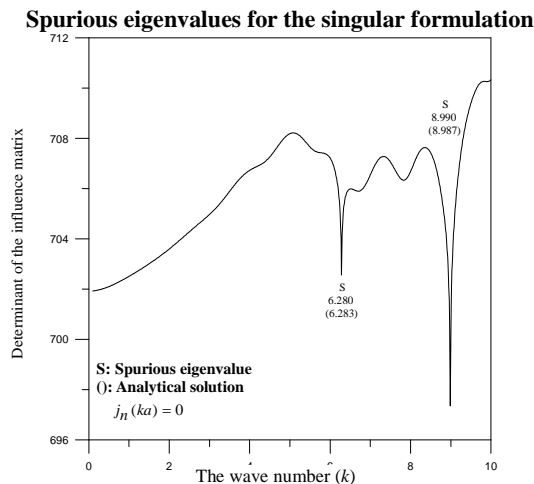
(d) Determinant versus the wave number by using the hypersingular formulation subject to the Dirichlet condition.



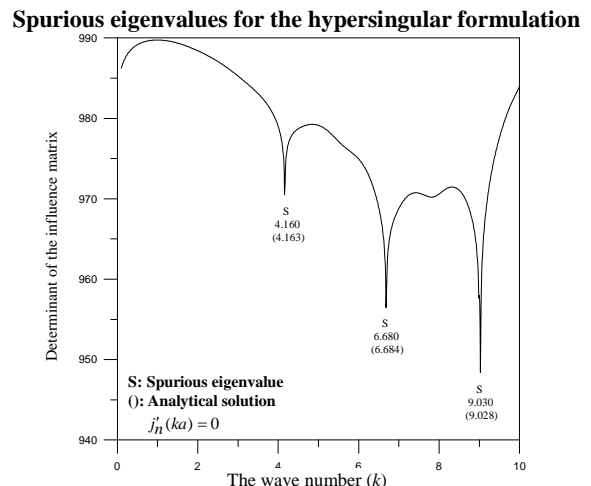
(b) Determinant versus the wave number by using the singular formulation subject to the Neumann condition.



(e) Determinant versus the wave number by using the hypersingular formulation subject to the Neumann condition.



(c) Extraction of the spurious eigenvalues for the singular formulation by using the SVD updating document.



(f) Extraction of the spurious eigenvalues for the hypersingular formulation by using the SVD updating document.

Figure 2-5 Extraction of spurious eigenvalues for a concentric sphere by using the SVD updating documents ($a = 0.5$ and $b = 1.0$).

Chapter 3 Eigenproblems with a multiply-connected domain by using the multipole Trefftz method

Summary

In this chapter, 2D eigenproblems with the multiply-connected domain are studied by using the multipole Trefftz method. We extend the conventional Trefftz method to the multipole Trefftz method by introducing the multipole expansion. The addition theorem is employed to expand the Trefftz bases to the same polar coordinates centered at one circle, where boundary conditions are specified. Owing to the introduction of the addition theorem, collocation technique isn't required to construct the linear algebraic system. The eigenvalues can be found by employing the SVD. To deal with the eigenproblems by using the present method is free of pollution of spurious eigenvalues. Both the eigenvalues and eigenmodes are compared well with the analytical solutions and those of BEM for illustrative examples.

3.1 Introduction

Eigenproblems become more and more important issues in new product design process. Many scholars have studied the sound radiation behavior and tried to find the connection between the sound radiation and vibration. They aimed to find an approach to decouple the sound radiation. Many well-developed numerical methods such as the finite element method (FEM), finite difference method (FDM) and boundary element method (BEM) can be adopted. Especially, the BEM has become popular in recent years due to its advantage of the reduction of dimensionality. However, spurious and fictitious frequencies occur and stem from non-uniqueness solution problems. They appear in different aspects on computational mechanics. For example, hourglass modes in the FEM using the reduced integration occur due to the rank deficiency (Winkler and Davies, 1984). Also, loss of divergence-free constraint for the incompressible elasticity also results in spurious modes. In the other aspect of numerical solution for the differential equation using the FDM, the spurious eigenvalue also appears due to discretization (Greenberg, 1998; Fujiwara, 1998; Zhao, 2007). If the incomplete set is adopted in the solution representation such as the real-part BEM (Kuo et al., 2000) or

the multiple reciprocity method (MRM; Chen and Wong, 1997; Chen and Wong, 1998; Yeih et al., 1998; Yeih et al., 1999(a)(b); Chen et al., 2003(a)), spurious eigensolutions occur in solving eigenproblems with simply-connected domain. Even though the complex-valued kernel is adopted in BEM, the spurious eigensolution also occurs for multiply-connected problems (Chen et al., 2003(b)) as well as the appearance of fictitious frequency for exterior acoustics (Chen et al., 2006(a)). Spurious solutions and fictitious frequencies in the integral formulation belong to spectral pollution since it cannot be suppressed by refining the mesh. The origin of spurious modes arises from an improper approximation of null space of the integral operator (Schroeder, 1994). This chapter focuses on finding a meshless method free of spurious eigenvalue.

In the recent years, the meshless methods started to capture the interest of the researchers in the community of computational mechanics because these methods are mesh free and only boundary nodes are necessary (Young et al., 2005; Chen et al., 2006(b); Atluri et. al., 1999; Atluri and Shen, 2002). Among meshless methods, the Trefftz method is a boundary-type solution procedure using only the T-complete functions satisfying the governing equation (Li et al., 2008). Since Trefftz presented the Trefftz method for solving boundary value problems in 1926 (Trefftz, 1926), various Trefftz methods such as direct formulations and indirect formulations (Kita and Kamiya, 1995) have been developed. The key issue in the use of the indirect Trefftz method is the definition of T-complete function set, which ensures the convergence of the subsequent field variable expansions towards the analytical solutions. Many applications to the Laplace equation (Karageorghis and Fairweather, 1999), the Helmholtz equation (Fairweather and Karageorghis, 1998), the Navier equation (Jin et al., 1990 and 1993) and the biharmonic equation (Jirousek and Wroblewski, 1996) were done. Readers can consult with the Li et al.'s book (Li et al., 2008). However, all the applications seemed to be limited on simply-connected domains. The concept of multipole method to solve exterior problems was firstly devised by Závěška (1913) and used for the interaction of waves with arrays of circular cylinders by Linton and Evans (1990). Recently, Martin (2006) reviewed several methods to solve problems of the multiple scattering in acoustics, electromagnetism, seismology and hydrodynamics. However, the interior eigenproblems were not mentioned therein. Extension to interior multiply-connected problems by using the multipole Trefftz method is also our concern

of this chapter.

This chapter employs the addition theorem to expand the Bessel (J) and Hankel (H) functions (Graf, 1893) in the solution representation for matching the boundary conditions in an analytical way. The so-called multipole Trefftz technique is analytical and effective in solving problems with the multiply-connected domain. Numerical experiments were performed to verify the present method. For the multiply-connected problem, the mode shapes were plotted by using the multipole Trefftz method and were compared with the other available results, e.g. exact solutions and BEM data (Chen et al., 2001; Chen et al., 2004).

3.2 Multipole Trefftz method for multiply-connected problems with circular boundaries

3.2.1 Problem statement

The governing equation for the eigenproblem is the Helmholtz equation as follows:

$$\left(\nabla^2 + k^2\right)u(\mathbf{x}) = 0, \mathbf{x} \in D, \quad (3-1)$$

where ∇^2 , k and D are the Laplacian operator, the wave number and the domain of interest, respectively. The multiply-connected domain with circular boundaries is depicted in Fig. 3-1. The radius of the j th circle and the position vector of its center are R_j and \mathbf{O}_j , respectively.

3.2.2 Conventional Trefftz method for the simply-connected domain

In the Trefftz method, the field solution $u(\mathbf{x})$ for a simply-connected domain is superimposed by the T-complete functions, $\varphi_m(\mathbf{x})$, as follows:

$$u(\mathbf{x}) = \sum_{m=-M}^M \alpha_m \varphi_m(\mathbf{x}), \quad (3-2)$$

where $\varphi_m(\mathbf{x})$ is the Trefftz base with respect to the origin O , $(2M + 1)$ is the number of complete functions and α_m is the m th unknown coefficient which can be determined by matching the boundary conditions. This chapter focuses on problems with a circular boundary, so the polar coordinates are utilized and the field point \mathbf{x} is expressed as $\mathbf{x} = (\rho, \phi)$. For the circular boundary with a radius R , the complete

functions for 2D Helmholtz problems are shown below:

$$\varphi_m = \begin{cases} \varphi_m^I(\rho, \phi) = J_m(k\rho)e^{im\phi}, \rho < R, & \text{interior case, } m = 0, \pm 1, \pm 2, \dots, M, \\ \varphi_m^E(\rho, \phi) = H_m^{(1)}(k\rho)e^{im\phi}, \rho > R, & \text{exterior case, } m = 0, \pm 1, \pm 2, \dots, M, \end{cases} \quad (3-3)$$

where the superscripts of “ I ” and “ E ” denote the interior and exterior domains, respectively.

3.2.3 Graf's addition theorem

According to the Graf's addition theorem (Graf, 1893) for $J_m(k\rho_p)e^{im\phi_p}$ and $H_m^{(1)}(k\rho_p)e^{im\phi_p}$, we have

$$\begin{aligned} J_m(k\rho_p)e^{im\phi_p} &= \sum_{n=-\infty}^{\infty} J_{m-n}(kb_{pq})e^{i(m-n)\theta_{pq}} J_n(k\rho_q)e^{in\phi_q} \\ &= \sum_{n=-\infty}^{\infty} J_{m-n}(k\rho_q)e^{i(m-n)\phi_q} J_n(kb_{pq})e^{in\theta_{pq}}, \end{aligned} \quad (3-4)$$

$$H_m^{(1)}(k\rho_p)e^{im\phi_p} = \begin{cases} \sum_{n=-\infty}^{\infty} J_{m-n}(kb_{pq})e^{i(m-n)\theta_{pq}} H_n^{(1)}(k\rho_q)e^{in\phi_q}, & b_{pq} < \rho_q \\ \sum_{n=-\infty}^{\infty} H_{m-n}^{(1)}(kb_{pq})e^{i(m-n)\theta_{pq}} J_n(k\rho_q)e^{in\phi_q}, & b_{pq} > \rho_q \end{cases}, \quad (3-5)$$

where (b_{pq}, θ_{pq}) is the position vector (the polar coordinates) of the q th center with respect to the p th center as shown in Fig. 3-2.

3.2.4 Multipole Trefftz method

Since the multiply-connected domain is considered, both the interior and exterior complete functions are required. The field solution can be represented by

$$u(\mathbf{x}; \rho_0, \phi_0, \rho_1, \phi_1, \dots, \rho_N, \phi_N) = \sum_{m=-\infty}^{\infty} \alpha_m^0 J_m(k\rho_0)e^{im\phi_0} + \sum_{j=1}^N \sum_{m=-\infty}^{\infty} \alpha_m^j H_m^{(1)}(k\rho_j)e^{im\phi_j}, \quad (3-6)$$

where α_m^j is the unknown coefficient of the m th complete function for \mathbf{O}_j and the position vector of the field point \mathbf{x} with respect to \mathbf{O}_j is noted (ρ_j, ϕ_j) , $j = 0, 1, 2, \dots, N$. as shown in Fig. 3-3. In order to enforce the boundary condition on B_0

($\rho_0 = R_0$), we must express each term as a function of (R_0, ϕ_0) for the solution representation. By translating $H_m^{(1)}(k\rho_n)e^{im\phi_n}$ in terms of functions of (ρ_0, ϕ_0) using the addition theorem of Eq. (3-5), we have

$$\begin{aligned}
u(\mathbf{x}; R_0, \phi_0) &= \sum_{m=-\infty}^{\infty} \alpha_m^0 J_m(kR_0) e^{im\phi_0} \\
&+ \sum_{j=1}^N \sum_{m=-\infty}^{\infty} \alpha_m^j \sum_{n=-\infty}^{\infty} J_{m-n}(kb_{j0}) e^{i(m-n)\theta_{j0}} H_n^{(1)}(kR_0) e^{in\phi_0}, \quad x \in B_0,
\end{aligned} \tag{3-7}$$

where j , m and n in the three summation symbols denote indexes of the number of the circular holes, number of the Trefftz bases and number of terms in the addition theorem, respectively. For the Dirichlet problem, the boundary condition on B_0 is $\bar{u}_0 = 0$. By comparing the coefficient of $e^{im\phi_0}$, we have

$$\alpha_m^0 J_m(kR_0) + H_m^{(1)}(kR_0) \sum_{j=1}^N \sum_{n=-\infty}^{\infty} \alpha_n^j J_{n-m}(kb_{j0}) e^{i(n-m)\theta_{j0}} = 0, \quad m = 0, \pm 1, \pm 2, \dots \tag{3-8}$$

If we consider to enforce the boundary condition on B_l ($\rho_l = R_l$), $J_m(k\rho_0) e^{im\phi_0}$ and $H_m^{(1)}(k\rho_j) e^{im\phi_j}$, $j = 1, 2, \dots, N$ and $j \neq l$, in Eq. (3-6) are required to translate into (ρ_l, ϕ_l) system using the addition theorem. The field solution of Eq. (3-6) yields

$$\begin{aligned}
u(\mathbf{x}; R_l, \phi_l) &= \sum_{m=-\infty}^{\infty} \alpha_m^0 \sum_{n=-\infty}^{\infty} J_n(kR_l) e^{in\phi_l} J_{m-n}(kb_{0l}) e^{i(m-n)\theta_{0l}} + \sum_{m=-\infty}^{\infty} \alpha_m^l H_m^{(1)}(kR_l) e^{im\phi_l} \\
&+ \sum_{\substack{j=1 \\ j \neq l}}^N \sum_{m=-\infty}^{\infty} \alpha_m^j \sum_{n=-\infty}^{\infty} f_{mn}(R_l, \phi_l, b_{jl}, \theta_{jl}), \quad x \in B_l,
\end{aligned} \tag{3-9}$$

where

$$f_{mn}(R_l, \phi_l, b_{jl}, \theta_{jl}) = \begin{cases} H_n^{(1)}(kR_l) e^{in\phi_l} J_{m-n}(kb_{jl}) e^{i(m-n)\theta_{jl}}, & b_{jl} < R_l \\ J_n(kR_l) e^{in\phi_l} H_{m-n}^{(1)}(kb_{jl}) e^{i(m-n)\theta_{jl}}, & b_{jl} > R_l \end{cases}. \tag{3-10}$$

By satisfying the boundary condition $\bar{u}_l = 0$ and comparing with coefficients, we have

$$\begin{aligned}
J_m(kR_l) \sum_{n=-\infty}^{\infty} \alpha_n^0 J_{n-m}(kb_{0l}) e^{i(n-m)\theta_{0l}} + \alpha_m^l H_m^{(1)}(kR_l) \\
+ \sum_{\substack{j=1 \\ j \neq l}}^N \sum_{n=-\infty}^{\infty} \alpha_n^j f_{mn}(R_l, \phi_l, b_{jl}, \theta_{jl}) e^{-im\phi_l} = 0, \quad m = 0, \pm 1, \pm 2, \dots
\end{aligned} \tag{3-11}$$

Equations (3-8) and (3-11) form a system of equations of simultaneous linear algebraic equations for the coefficients α_m^0 and α_m^j , $m = 0, \pm 1, \pm 2, \dots, \pm M$ and $n = 0, \pm 1, \pm 2, \dots, \pm M$, as shown below:

$$[\Phi]_{[(N+1) \times (2M+1)] \times [(N+1) \times (2M+1)]} \{\mathbf{c}\}_{[(N+1) \times (2M+1)] \times 1} = \{0\}, \tag{3-12}$$

where

$$[\Phi] = \begin{bmatrix} \Phi_{00} & \Phi_{01} & \cdots & \Phi_{0N} \\ \Phi_{10} & \Phi_{11} & \cdots & \Phi_{1N} \\ \vdots & \vdots & \ddots & \vdots \\ \Phi_{N0} & \Phi_{N1} & \cdots & \Phi_{NN} \end{bmatrix}, \quad (3-13)$$

$$\{\mathbf{c}\} = \begin{Bmatrix} \mathbf{c}_0 \\ \mathbf{c}_1 \\ \vdots \\ \mathbf{c}_N \end{Bmatrix}. \quad (3-14)$$

in which $[\Phi]$ is dimension of $(N+1) \times (2M+1)$ by $(N+1) \times (2M+1)$, $\{\mathbf{c}\}$ denotes the column vector of unknown coefficients with a dimension of $(N+1) \times (2M+1)$ by 1. The submatrix, $[\Phi_{pq}]$, denotes the potential of the q th circular boundary respect to O_p . $[\Phi_{pq}]$ can be written as

$$[\Phi_{pq}] = \begin{cases} \begin{bmatrix} J_{-M}(kR_0)e^{-iM\phi_0} & 0 & 0 & 0 \\ 0 & J_{-M+1}(kR_0)e^{i(-M+1)\phi_0} & 0 & 0 \\ 0 & 0 & \ddots & 0 \\ 0 & 0 & 0 & J_M(kR_0)e^{iM\phi_0} \end{bmatrix}, & p = q = 0, \\ \begin{bmatrix} H_{-M}^{(1)}(kR_p)e^{-iM\phi_p} & 0 & 0 & 0 \\ 0 & H_{-M+1}^{(1)}(kR_p)e^{i(-M+1)\phi_p} & 0 & 0 \\ 0 & 0 & \ddots & 0 \\ 0 & 0 & 0 & H_M^{(1)}(kR_p)e^{iM\phi_p} \end{bmatrix}, & p = q \neq 0, \\ \begin{bmatrix} J_{-M}(kR_p)e^{-iM\phi_p} J_{-M+M}(kb_{0p})e^{i(-M+M)\theta_{0p}} & \cdots & J_{-M}(kR_p)e^{-iM\phi_p} J_{-M-M}(kb_{0p})e^{i(-M-M)\theta_{0p}} \\ \vdots & \ddots & \vdots \\ J_M(kR_p)e^{iM\phi_p} J_{M+M}(kb_{0p})e^{i(M+M)\theta_{0p}} & \cdots & J_M(kR_p)e^{iM\phi_p} J_{M-M}(kb_{0p})e^{i(M-M)\theta_{0p}} \end{bmatrix}, & p \neq 0 \text{ and } q = 0 \\ \begin{bmatrix} H_{-M}^{(1)}(kR_p)e^{-iM\phi_p} J_{-M+M}(kb_{qp})e^{i(-M+M)\theta_{qp}} & \cdots & H_{-M}^{(1)}(kR_p)e^{-iM\phi_p} J_{-M-M}(kb_{qp})e^{i(-M-M)\theta_{qp}} \\ \vdots & \ddots & \vdots \\ H_M^{(1)}(kR_p)e^{iM\phi_p} J_{M+M}(kb_{qp})e^{i(M+M)\theta_{qp}} & \cdots & H_M^{(1)}(kR_p)e^{iM\phi_p} J_{M-M}(kb_{qp})e^{i(M-M)\theta_{qp}} \end{bmatrix}, & \text{otherwise.} \end{cases} \quad (3-15)$$

Moreover, the gradient of $u(\mathbf{x})$ is

$$\begin{aligned}\nabla u &= \nabla u(\mathbf{x}; \rho_0, \phi_0, \rho_1, \phi_1, \dots, \rho_N, \phi_N) \\ &= \nabla \left[\sum_{m=-\infty}^{\infty} \alpha_m^0 J_m(k\rho_0) e^{im\phi_0} + \sum_{j=1}^N \sum_{m=-\infty}^{\infty} \alpha_m^j H_m^{(1)}(k\rho_j) e^{im\phi_j} \right].\end{aligned}\quad (3-16)$$

For the Neumann problem, we have the normal derivative

$$\begin{aligned}\nabla u \cdot \mathbf{n}_x &= \nabla \left[\sum_{m=-\infty}^{\infty} \alpha_m^0 J_m(k\rho_0) e^{im\phi_0} + \sum_{j=1}^N \sum_{m=-\infty}^{\infty} \alpha_m^j H_m^{(1)}(k\rho_j) e^{im\phi_j} \right] \cdot \mathbf{n}(\mathbf{x}), \\ & \quad m = 0, \pm 1, \pm 2, \dots\end{aligned}\quad (3-17)$$

For satisfying the boundary conditions on $B_0(t_0 = 0)$ and $B_l(t_l = 0)$ and comparing with coefficients, we have

$$\begin{aligned}\alpha_m^0 J'_m(kR_0) + H_m^{(1)'}(kR_0) \sum_{j=1}^N \sum_{n=-\infty}^{\infty} \alpha_n^j J_{n-m}(kb_{j0}) e^{i(n-m)\theta_{j0}} &= 0, \\ & m = 0, \pm 1, \pm 2, \dots, \pm M \text{ and } \mathbf{x} \in B_0\end{aligned}\quad (3-18)$$

and

$$\begin{aligned}J'_m(kR_l) \sum_{n=-\infty}^{\infty} \alpha_n^0 J_{n-m}(kb_{0l}) e^{i(n-m)\theta_{0l}} + \alpha_m^l H_m^{(1)'}(kR_l) \\ + \sum_{\substack{j=1 \\ j \neq l}}^N \sum_{n=-\infty}^{\infty} \alpha_n^j \frac{\partial}{\partial \rho_l} f_{nm}(\rho_l, \phi_l, b_{jl}, \theta_{jl}) e^{-im\phi_l} \Bigg|_{\rho_l=R_l} &= 0, \\ & m = 0, \pm 1, \pm 2, \dots, \pm M, \mathbf{x} \in B_l, l = 1, 2, \dots, N.\end{aligned}\quad (3-19)$$

Equations (3-18) and (3-19) form a system of simultaneous linear algebraic equations for the coefficients α_m^0 and α_m^j , $m = 0, \pm 1, \pm 2, \dots$. By applying the SVD technique for the matrix $[\Phi]$, the determinant versus k is used to detect eigenvalues and nontrivial vector of $\{\mathbf{c}\}$. The eigenmode is obtained by searching the right unitary vector for $\{\mathbf{c}\}$ corresponding to the zero singular value. The number of the zero singular values implies the multiplicity of roots.

3.3 Illustrative examples

We consider two cases of Helmholtz eigenproblem with a multiply-connected domain subjected to the Dirichlet boundary conditions.

Case 1: a circular membrane with eccentric hole (special case: annulus)

The eccentric domain is shown in Table 3-1. The radii of the outer and inner circular

boundaries are $R_0 = 2$ and $R_1 = 0.5$, respectively. The eccentricity $e = b_{01} = b_{10}$ is 0.5. Both the boundary conditions are $\bar{u}_j = 0, j = 0, 1$. Extraction of eigenvalues free of pollution of spurious eigenvalues by using the SVD technique is shown in Fig. 3-4. The eigenvalues and modes can be obtained as shown in Tables 3-1 and 3-2. The results of this approach agree well with those of BEM (Chen et al., 2001).

A special case of eccentric ring is an annular domain which is also considered in Table 3-1 and the radii of the outer and inner circles are the same as the eccentric case. The two circles are concentric hence the distance between the two poles is zero ($b_{01} = b_{10} = 0$). The linear algebraic system reduces to that derived by the conventional Trefftz method. Moreover, the analytical solution could be derived by using this approach. Eqs. (3-8) and (3-11) can be rewritten as

$$\alpha_m^0 J_m(kR_0) + \alpha_m^1 H_m^{(1)}(kR_0) = 0, m = 0, \pm 1, \pm 2, \dots \pm \infty, \quad (3-20)$$

$$\alpha_m^0 J_m(kR_1) + \alpha_m^1 H_m^{(1)}(kR_1) = 0, m = 0, \pm 1, \pm 2, \dots \pm \infty. \quad (3-21)$$

According to Eqs. (3-20) and (3-21), the analytical equation is found as below:

$$J_m(kR_0)Y_m(kR_1) - J_m(kR_1)Y_m(kR_0) = 0, m = 0, \pm 1, \pm 2, \dots \pm \infty, \quad (3-22)$$

where Y_m is the Bessel function of the second kind. The analytical eigenvalues are also shown in Table 3-1. By using the SVD technique, the determinant of the influence matrix versus the wave number is shown in Fig. 3-5. The true eigenvalues and modes are shown in Tables 3-1 and 3-3, respectively. Although the mode shape corresponding to the eigenvalues k_2 and k_3 seem different from the results of the BEM, mode shapes of the present method can be linearly superimposed by using the two independent mode shapes of BEM, and vice versa.

Case 2: a circular membrane with four circular holes

The outer boundary with a radius $R_0 = 1$ and four holes of equal size with radii $R_j = 0.1, j = 1, 2, 3, 4$ are considered and the former five eigenvalues are shown in Table 3-4. The positions of the four centers of the circular holes are $(0.5, 0), (0, 0.5), (-0.5, 0)$ and $(0, -0.5)$. Chen et al. (2004) also used the BEM for finding the eigenvalues of Dirichlet problems. The eigenvalues extracted out by the

SVD are shown in Fig. 3-6. Eigenvalues and eigenmodes using BEM and the present method are shown in Tables 3-4 and 3-5, respectively. Although the shapes of modes 2 and 3 seem different from the results of the BEM, mode shapes of the present method can be linearly superimposed by using the two independent mode shapes of BEM, and vice versa. Good agreement is made.

3.4 Conclusions

In this chapter, the Graf's addition theorem was used to reform the awkward situation of the classical Trefftz method for multiply-connected problems. This approach was coined the multipole Trefftz method. The multipole Trefftz method has successively provided an analytical model for solving eigenvalues and eigenmodes of a circular membrane containing multiple circular holes. The numerical experiments of the multiply-connected problems were performed to demonstrate the validity of the present approach. Good agreements between the results of the multipole Trefftz method and the BEM were made. In addition, the ability of detecting the multiplicity of roots can be achieved in the multipole Trefftz method by using the SVD technique free of pollution of spurious eigenvalues. Numerical results show high accuracy and fast rate of convergence thanks to the analytical approach.

Table 3-1 The first five eigenvalues for a multiply-connected problem with an eccentric annulus and a concentric annulus using different approaches.

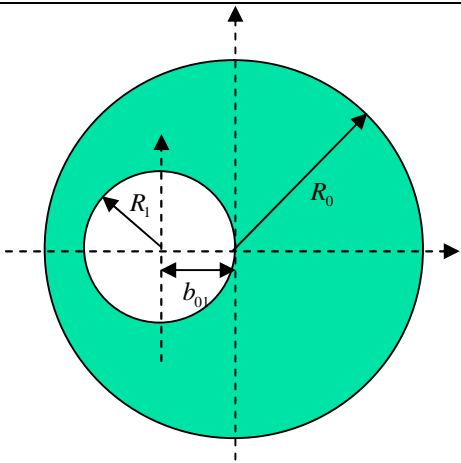
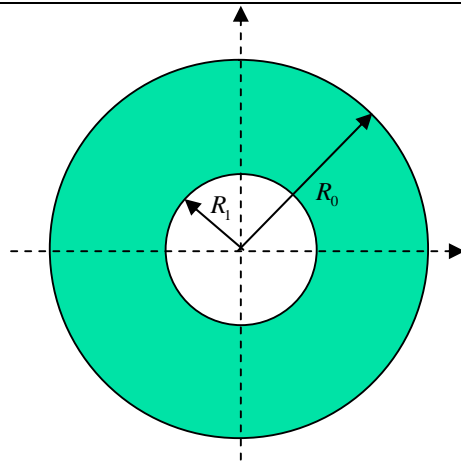
	eccentric annulus		concentric annulus		
					
	Multipole Trefftz method	BEM (Chen et al. 2001)	Multipole Trefftz method	BEM (Chen et al., 2001)	Analytical solution
k_1	1.74	1.75	2.05	2.06	2.04884
k_2	2.13	2.14	2.22	2.23	2.22375
k_3	2.46	2.47	2.22	2.23	2.22375
k_4	2.77	2.78	2.66	2.67	2.65993
k_5	2.96	2.98	2.66	2.67	2.65993

Table 3-2 The first five modes for a multiply-connected problem with an eccentric hole.

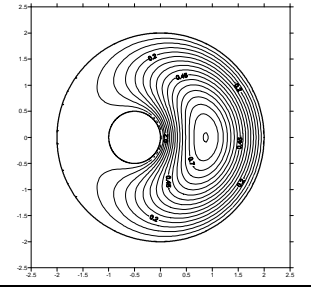
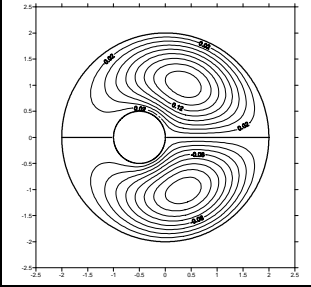
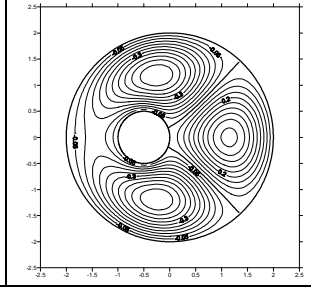
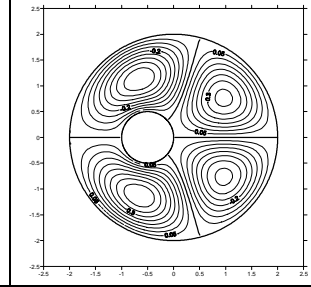
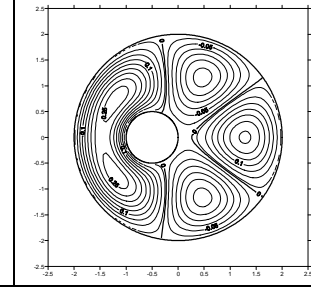
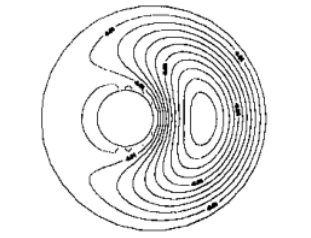
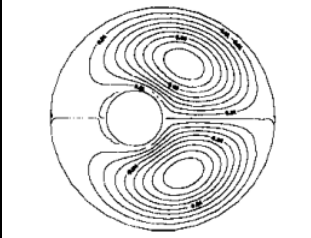
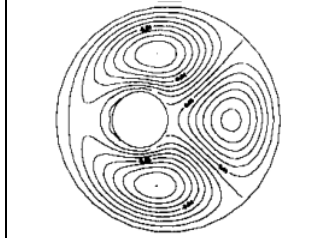
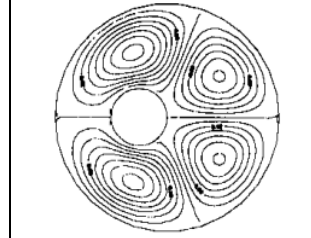
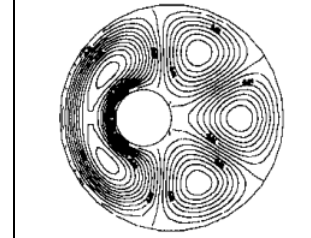
Mode No.	1	2	3	4	5
eigenvalue	1.74	2.13	2.46	2.77	2.96
Multipole Trefftz method					
eigenvalue	1.74	2.14	2.47	2.78	2.97
BEM (Chen et al., 2001)					

Table 3-3 The first five modes for a multiply-connected problem with a concentric hole.

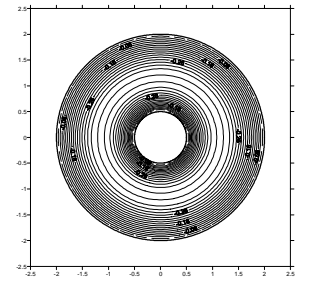
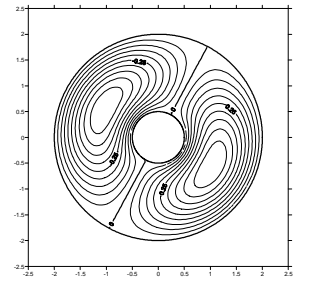
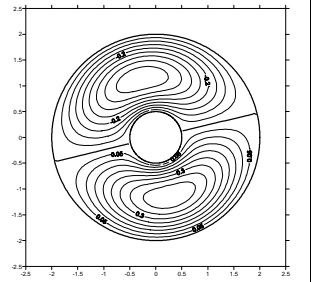
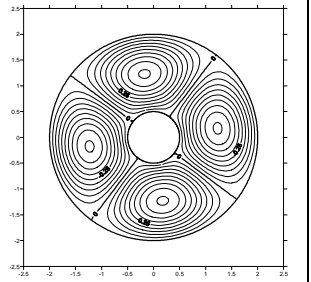
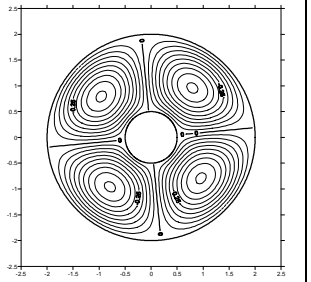
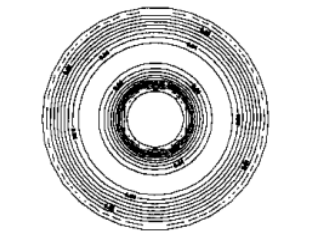
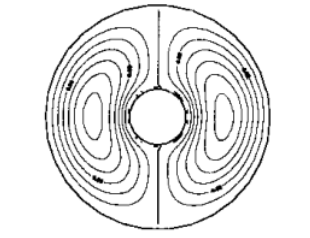
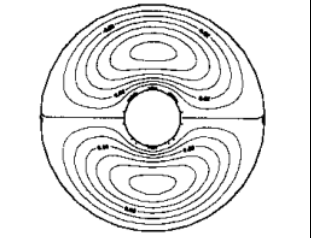
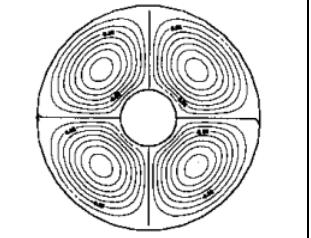
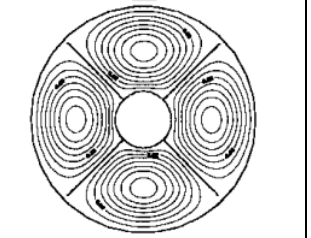
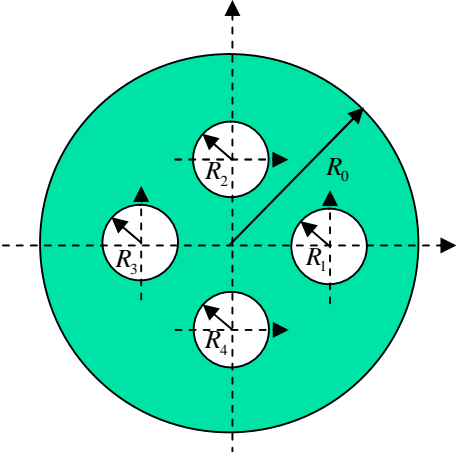
Mode No.	1	2	3	4	5
eigenvalue	2.05	2.22	2.22	2.66	2.66
Multipole Trefftz method					
eigenvalue	2.06	2.23	2.23	2.67	2.67
BEM (Chen et al., 2001)					

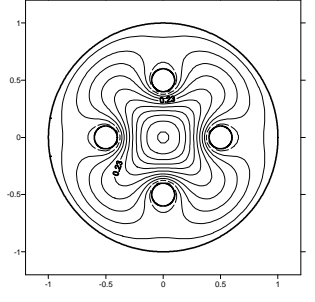
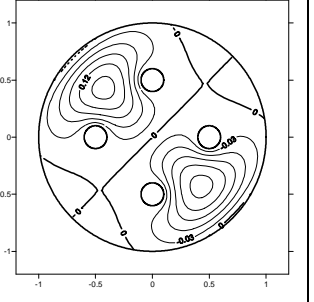
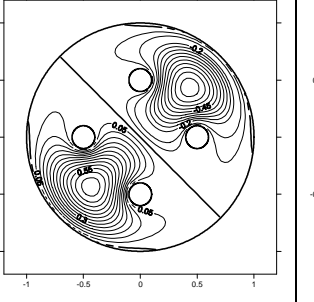
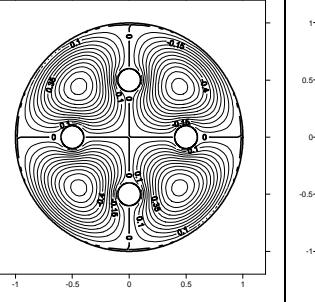
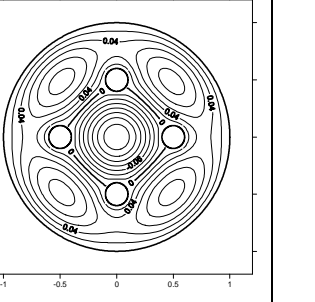
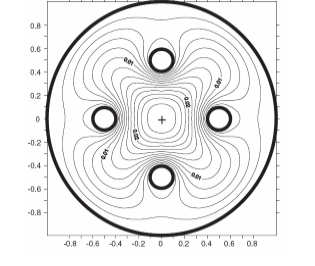
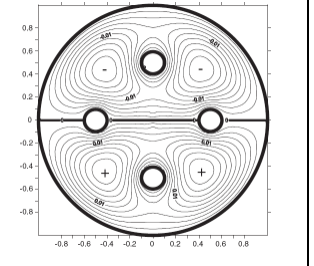
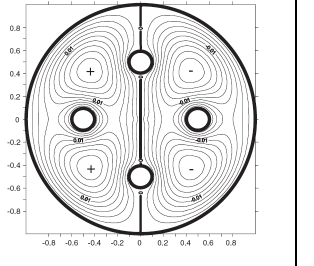
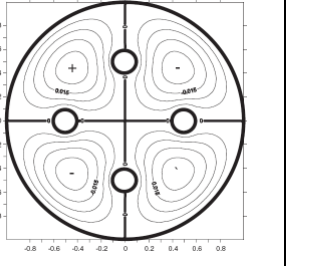
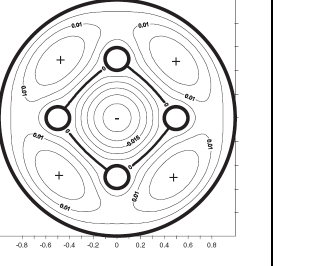
Table 3-4 The first five eigenvalues for a multiply-connected problem with four equal holes using different approaches.



The diagram shows a large green circle representing a domain. Inside this domain are four smaller white circles representing holes, arranged symmetrically around the center. The holes are labeled R_0 , R_1 , R_2 , and R_4 . A horizontal dashed line and a vertical dashed line intersect at the center, representing the coordinate axes. Arrows point from the center to the centers of the holes, labeled R_0 , R_1 , R_2 , and R_4 . The hole R_0 is in the first quadrant, R_1 is on the positive x-axis, R_2 is in the second quadrant, and R_4 is on the negative x-axis.

	Multipole Trefftz method	BEM (Chen et al., 2004)
k_1	4.499	4.47
k_2	5.369	5.37
k_3	5.369	5.37
k_4	5.549	5.54
k_5	5.949	5.95

Table 3-5 The first five modes for a multiply-connected problem with four equal holes.

Mode No.	1	2	3	4	5
eigenvalue	4.499	5.369	5.369	5.549	5.949
Multipole Trefftz method					
eigenvalue	4.47	5.37	5.37	5.54	5.95
BEM (Chen et al., 2004)					

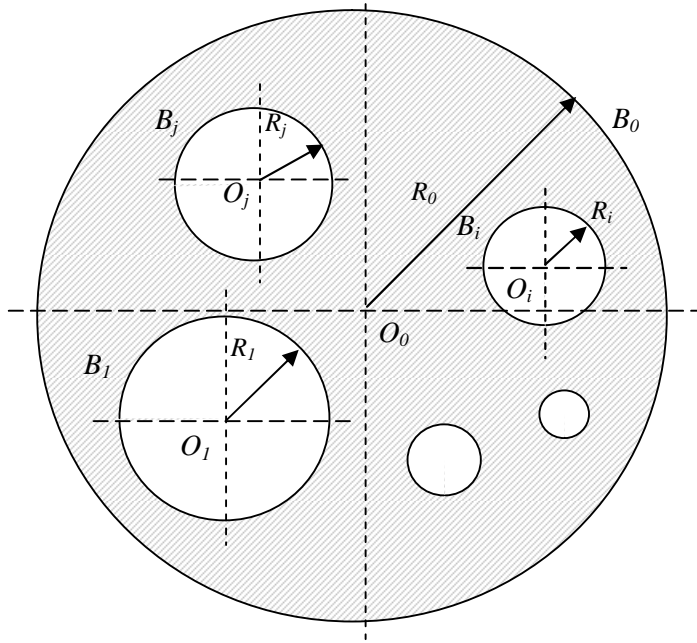


Figure 3-1 A multiply-connected domain with circular boundaries

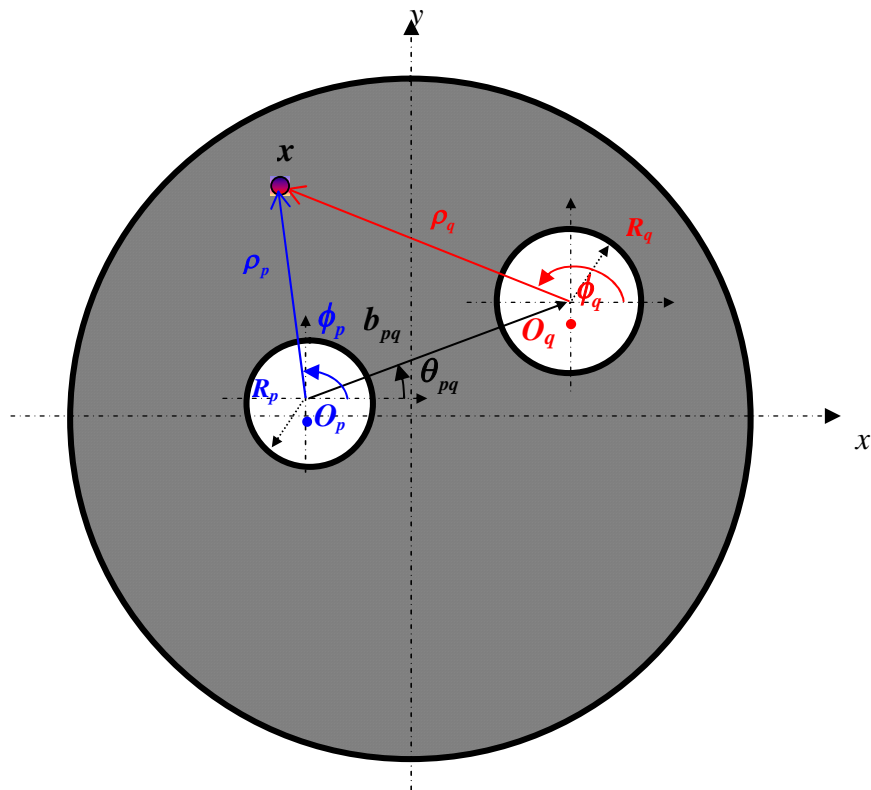


Figure 3-2 Notations of the Graf's addition theorem

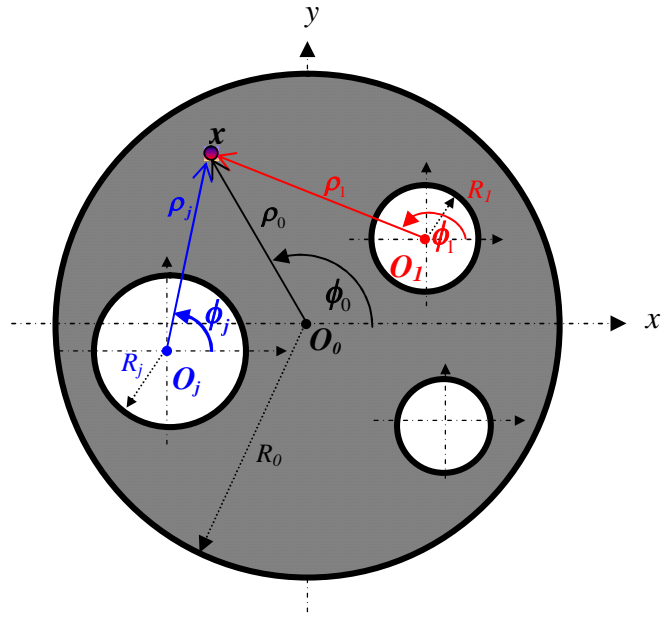


Figure 3-3 Notations in the multipole Trefftz method

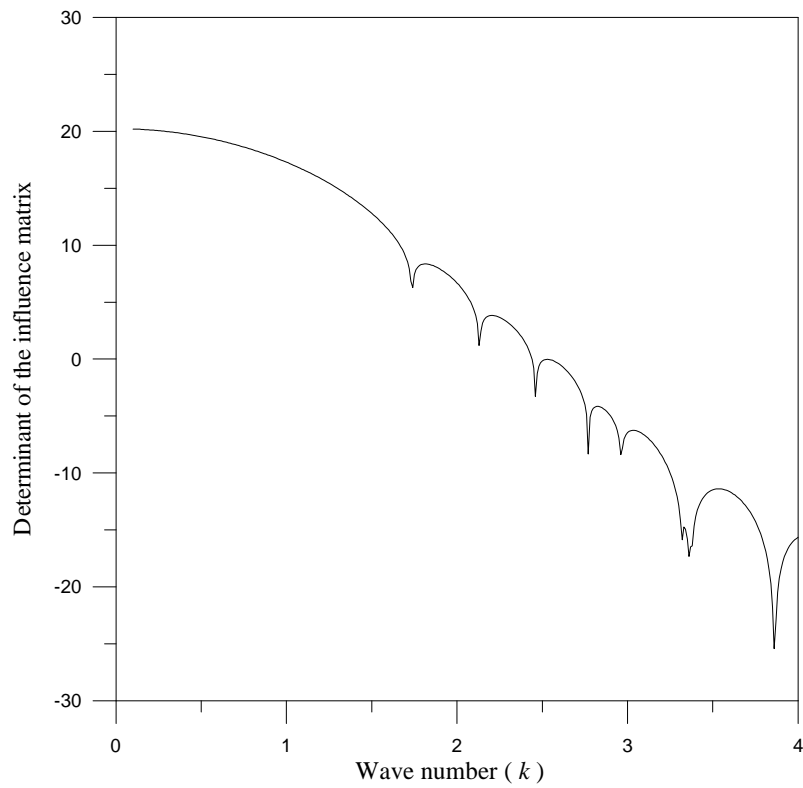


Figure 3-4 Determinant versus the wave number by using the multipole Trefftz method for the eccentric case

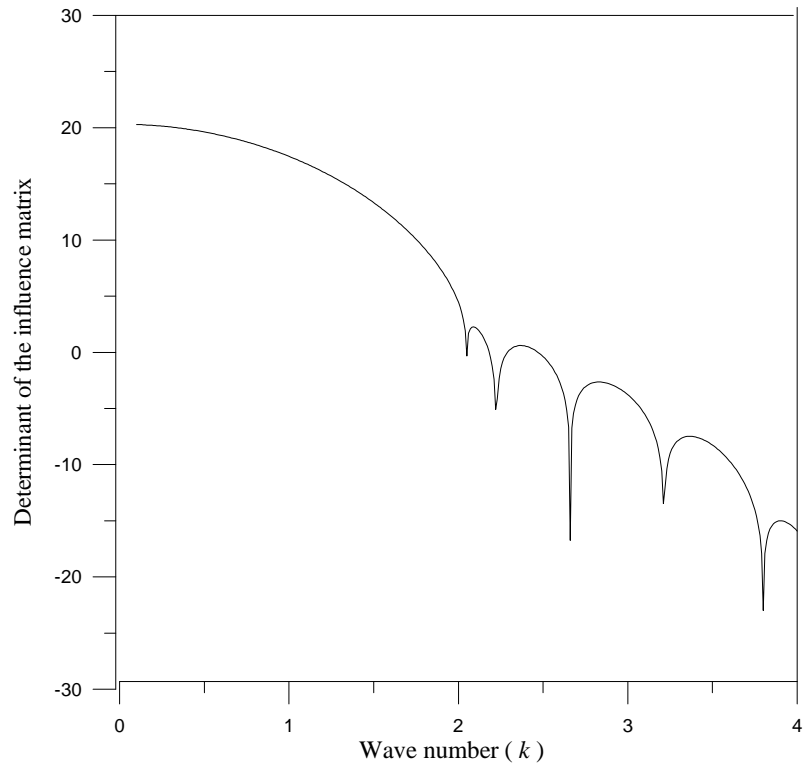


Figure 3-5 Determinant versus the wave number by using the multipole Trefftz method for the concentric case

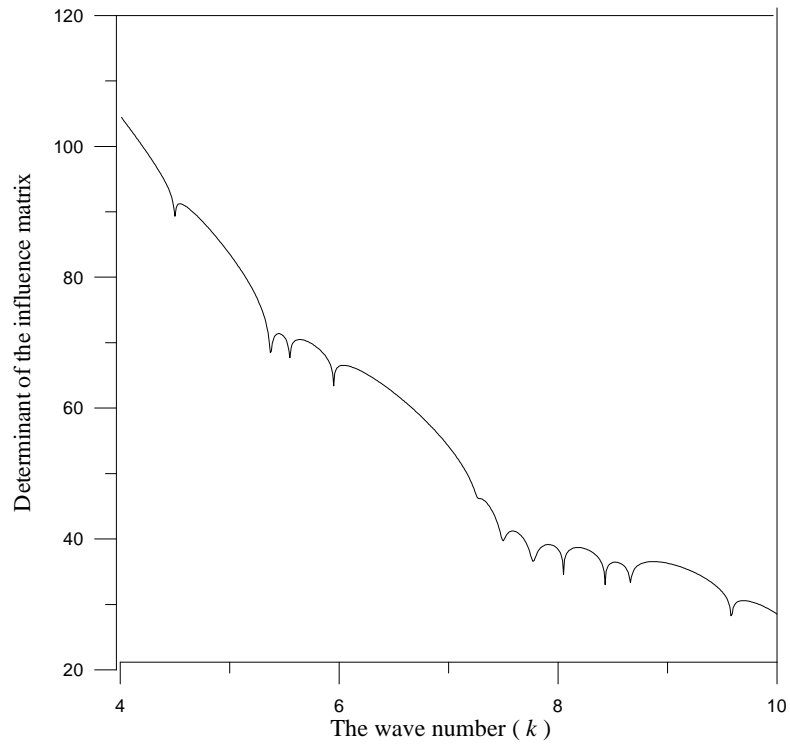


Figure 3-6 Determinant versus the wave number by using the multipole Trefftz method for the multiply-connected case with four equal holes

Chapter 4 Conclusions and further research

4.1 Conclusions

In this thesis, we solved eigenproblems by using two methods. One of the approaches is via the null-field integral equation emphasizing on the two issues of avoiding the singular and hypersingular integrals and the boundary-layer effect. The key idea is to approximate the boundary unknowns via truncated spherical harmonics on the spherical boundaries and to expand kernels of the integral operators into degenerate form. Those are the fundamental solution by truncating the addition theorem to have the degenerate kernels. The other one employed the addition theorem to expand the potential free of the adaptive observer system and the tensor transformation technique. Based on the proposed formulations for solving the eigenproblems involving circular and spherical boundaries, some concluding remarks are drawn below. The first four items are the conclusions of the BIEM, while the other items are the points for the multipole Trefftz method.

1. A systematic approach to solve eigenproblems for Helmholtz equation with spherical boundaries was adopted in this thesis by using the null-field integral equation in conjunction with degenerate kernels and spherical harmonics.
2. Spurious eigenvalues of a concentric sphere case were studied analytically and numerically in BIEM. One example was demonstrated to see how the spurious eigenvalues occur in the concentric sphere. It's found that spurious eigenvalues depend on the inner boundary and are independent of the outer boundary.
3. By using the updating term and updating document of SVD technique, true and spurious eigenvalues can be extracted out, respectively. Besides, true and spurious boundary eigenvectors are imbedded in the right and left unitary vectors of the SVD structure in the influence matrices, respectively.

4. The trivial outer boundary densities were examined in case of the spurious eigenvalue which is found to be the true eigenvalue for the domain bounded by the inner boundary. We also examined the existence of spurious eigenvalue for a concentric sphere in an analytical way by using the degenerate kernels and the spherical harmonics.
5. Based on the successful experiences on multipole scattering in Martins' book, the conventional Trefftz method was extended to the multipole Trefftz method by introducing the addition theorem. The addition theorem is employed to expand the Trefftz bases to the same polar coordinates centered at one circle, where boundary conditions are specified.
6. The multipole Trefftz method has successively provided an analytical model for solving eigenvalues and eigenmodes of a circular membrane containing multiple circular holes. The numerical experiments of the multiply-connected problems were performed to demonstrate the validity of this approach.
7. In addition, the ability of detecting the eigenvalues of the 2-D multiply-connected eigenproblems was demonstrated in the multipole Trefftz method free of pollution of spurious eigenvalues. Numerical results show high accuracy thanks to the analytical approach.

4.2 Further research

In this thesis, the multipole Trefftz method and the null-field integral equation were both employed to deal with 2-D and 3-D eigenproblems, respectively. However, there are several issues which can be further studied.

1. In the thesis, the fundamental solutions are expanded in the polar and spherical coordinates and only problems with circular and spherical boundaries can be solved. For the general boundary, e.g. ellipse, it can be further investigated if the

kernel functions can be expanded to separate form by using the elliptical coordinates.

2. Following the success of applications in concentric sphere, it's straightforward to extend this approach to solve the eigenproblems of an eccentric sphere in conjunction with the adaptive observe system and vector decomposition technique.
3. Although 2-D multiply-connected problems were solved analytically and numerically by using the multipole Trefftz method in this thesis, the extension to solve 3-D eigenproblems may be possible.
4. Regarding the BIEM, singular center expansion for kernel function has been done. However, the adaptive observe system and vector decomposition technique are requested. A bi-center expansion technique may be suitable for the eccentric case in a more straightforward way free of the adaptive observe system and vector decomposition technique.

References

- [1] Ali A., Rajakumar C. and Yunus S.M., Advances in acoustic eigenvalue analysis using boundary element method. *Comp. Stru.* 1995; 56(5): 837-47.
- [2] Atluri S.N., Kim H.G. and Cho J.Y., A critical assessment of the truly meshless local Petrov–Galerkin (MLPG), and local boundary integral equation (LBIE) methods. *Comput Mech* 1999; 24: 348-72.
- [3] Atluri S.N. and Shen S., The meshless local Petrov–Galerkin (MLPG) method: a simple and less-costly alternative to the finite element and boundary element methods. *Comput Model Eng Sci* 2002; 3: 11-51.
- [4] Chen H.B., Lu P. and Schnack E. (: Regularized algorithms for the calculation of values on and near boundaries in 2D elastic BEM. *Engineering Analysis with Boundary Elements* 2001; 25: 851-76.
- [5] Chen I.L., Chen J.T., Lee W.M. and Kao S.K., Computer assisted proof of spurious eigensolution for annular and eccentric membranes. *Journal of Marine Science and Technology*, accepted, 2009.
- [6] Chen J.T. and Hong H.K., Dual boundary integral equations at a corner using contour approach around singularity. *Advances in Engineering Software* 1994, 21: 169-78.
- [7] Chen J.T. and Wong F.C., Analytical derivations for one-dimensional eigenproblems using dual boundary element method and multiple reciprocity method. *Engng. Anal. Bound. Elem.* 1997; 20: 25-33.
- [8] Chen J.T. and Wong F.C., Dual formulation of multiple reciprocity method for the acoustic mode of a cavity with a thin partition. *J. Sound. Vibr.* 1998; 217(1): 75-95.
- [9] Chen J.T., Lin J.H., Kuo S.R. and Chyuan S.W., Boundary element analysis for the Helmholtz eigenvalue problems with a multiply connected domain. *Proc. Roy. Soc. A* 2001; 457: 2521-546.
- [10] Chen J.T., Lee C.F. and Lin S.Y., A new point of view for the polar decomposition using singular value decomposition. *Int. J. Comp. Numer. Anal.* 2002; 2(3): 257-64.
- [11] Chen J.T., Kuo S.R., Chung I.L. and Huang C.X., Study on the true and spurious eigensolutions of two-dimensional cavities using the multiple reciprocity method. *Engng. Anal. Bound. Elem.* 2003(a); 27: 655-70.

- [12] Chen J.T., Liu L.W. and Hong H.K., Spurious and true eigensolutions of Helmholtz BIEs and BEMs for a multiply-connected problem. *Proc. Roy. Soc. A* 2003(b), 459: 1891-925.
- [13] Chen J.T., Liu L.W. and Chyuan S.W., Acoustic eigenanalysis for multiply-connected problems using dual BEM. *Commun. Numer. Meth. Engng* 2004; 20: 419-40.
- [14] Chen J.T., Chen I.L. and Chen K.H., Treatment of rank deficiency in acoustics using SVD. *J. Comp. Acous.* 2006(a); 14(2): 157-83.
- [15] Chen J.T., Shen W.C. and Chen P.Y., Analysis of circular torsion bar with circular holes using null-field approach. *Comput Model Eng Sci* 2006(b); 12: 109–19.
- [16] Chen J.T., Shen W.C. and Wu A.C., Null-field integral equations for stress field around circular holes under anti-plane shear. *Engng. Anal. Bound. Elem.* 2006(c), 30(3): 205-17.
- [17] Chen J.T., Chen C.T., Chen P.Y. and Chen I.L., A semi-analytical approach for radiation and scattering problems with circular boundaries. *Comput. Methods Appl. Mech. Engrg.* 2007, 196: 2751-64.
- [18] Chen J.T. and Chen P.Y., A semi-analytical approach for stress concentration of cantilever beams with holes under bending. *J. Mech.* 2007, 23(3): 211-21.
- [19] De Mey G., Calculation of Helmholtz equation by an integral equation. *Int. J. Numer. Meth. Engng.* 1976; 10: 59-66.
- [20] De Mey G., A simplified integral equation method for the calculation of eigenvalues of Helmholtz equation. *Int. J. Numer. Meth. Engng.* 1977; 11: 1340-42.
- [21] Fairweather G. and Karageorghis A., The method of fundamental solutions for elliptic boundary value problems. *Advances in Computational Mathematics* 1998; 9: 69–95.
- [22] Fujiwara H., High-accurate numerical computation with multiple-precision arithmetic and spectral method, unpublished report, 2007.
- [23] Guiggiani M., Hypersingular boundary integral equations have an additional free term. *Computational Mechanics* 1995; 16: 245-8.
- [24] Graf J.H., Ueber die addition und subtraction der argumente bei Bessel'schen functionen nebst einer anwendung. *Mathematische annalen* 1893; 43: 136-44.
- [25] Greenberg M.D., Advanced engineering mathematics, Second edition.

- Prentice-Hall, 1998.
- [26] Gray L.J. and Manne L.L., Hypersingular integrals at a corner. *Engineering Analysis with Boundary Elements* 1993; 11: 327-34.
- [27] Huang Q. and Cruse T.A., Some notes on singular integral techniques in boundary element analysis. *International Journal for Numerical Methods in Engineering* 1993; 36: 2643-2659.
- [28] Hsiao C.C., A semi-analytical approach for Stokes flow and plate problems with circular boundaries, Master Thesis 2005, *Department of Harbor and River Engineering, National Taiwan Ocean University, Taiwan.*
- [29] Jin W.G., Cheung Y.K. and Zienkiewicz O.C., Application of the Trefftz method in plane elasticity problems. *Int. J. Numer. Meth. Engng.* 1990; 30: 1147-61.
- [30] Jin W.G., Cheung Y.K. and Zienkiewicz O.C., Trefftz method for Kirchhoff plate bending problems. *Int. J. Numer. Meth. Engng.* 1993; 36: 765-81.
- [31] Jirousek J. and Wroblewski A., T-elements: State of the art and future trends. *Archives of Computational Methods in Engineering* 1996; 3-4.
- [32] Karageorghis A. and Fairweather G., The method of fundamental solutions for axisymmetric potential problems. *Int. J. Numer. Meth. Engng.* 1999; 44: 1653-69.
- [33] Kisu H. and Kawahara T.: Boundary element analysis system based on a formulation with relative quantity. *Boundary Elements X*, Brebbia CA, eds., *Springer-Verlag* 1988; 1: 111-21.
- [34] Kita E. and Kamiya N., Trefftz method: An overview, *Advances in Engineering software* 1995; 24: 3-12.
- [35] Kuo S.R., Chen J.T. and Huang C.X., Analytical study and numerical experiments for true and spurious eigensolutions of a circular cavity using the real-part dual BEM. *Int. J. Numer. Meth. Engng.* 2000; 48: 1401-22.
- [36] Li Z.C., Lu T. T., Hu H. Y. and Cheng A. H. D., *Trefftz and collocation methods*, UK: WIT, 2008.
- [37] Linton C. M. and Evans D. V., The interaction of waves with arrays of vertical circular cylinders. *Journal Fluid Mechanics* 1990; 215: 549-69.
- [38] Martin P. A., *Multiple scattering interaction of time-harmonic wave with N obstacles*, UK: Cambridge University, 2006.
- [39] Schroeder W., *The origin of spurious modes in numerical solutions of*

- electromagnetic field eigenvalue problems. *IEEE Trans Microwave Theory Tech* 1994; 42: 644-53.
- [40] Sladek V. and Sladek J., Elimination of the boundary layer effect in BEM computation of stresses. *Communications in Applied Numerical Methods* 1991; 7: 539-50.
- [41] Telles J.C.F., A self-adaptative coordinate transformation for efficient numerical evaluation of general boundary element integrals. *International Journal for Numerical Methods in Engineering* 1987; 24: 959-73.
- [42] Trefftz E., Ein Gegenstück zum Ritzschen Verfahrenen, Proc 2nd Int Cong Mech Zurich, 1926, 131-37.
- [43] Tsai C.C., Young D.L., Chen C.W. and Fan C.N., The method of fundamental solutions for eigenproblems in the domains with and without interior holes. *Proc. Roy. Soc. A* 2006; 462: 1443-66.
- [44] Winkler J.R. and Davies J.B., Elimination of spurious modes in finite element analysis, *J. Comp. Phy.* 1984; 56: 1-14.
- [45] Yeih W., Chen J.T., Chen K.H. and Wong F.C., A study on the multiple reciprocity method and complex-valued formulation for the Helmholtz equation. *Adv. Engng. Soft.* 1998; 29(1): 1-6.
- [46] Yeih W., Chang J.R., Chang C.M. and Chen J.T., Applications of dual MRM for determining the natural frequencies and natural modes of a rod using the singular value decomposition method. *Adv. Engng. Soft.* 1999(a); 30: 459-68.
- [47] Yeih W., Chen J.T. and Chang C.M., Applications of dual MRM for determining the natural frequencies and natural modes of an Euler-Bernoulli beam using the singular value decomposition method. *Engng. Anal. Bound. Elem.* 1999(b); 23: 339-60.
- [48] Young D.L., Chen K.H. and Lee C.W., Novel meshless method for solving the potential problems with arbitrary domain. *J Comput Phys* 2005; 209: 290-321.
- [49] Závěška, F., Über die Beugung elektromagnetischer Wellen an parallelen, unendlich langen Kreiszyllindern. *Annalen der Physik, 4 Folge* 1913; 40: 1023-56.
- [50] Zhao S., On the spurious solutions in the high-order finite difference methods for eigenvalue problems. *Comput. Methods Appl. Mech. Engrg.* 2007; 196: 5031-46.

基本資料與簡歷

中文姓名：高聖凱

英文姓名：Shing-Kai Kao

出生日期：民國 67 年 11 月 03 日

籍貫：台北市

聯絡地址：台北市文山區景福街 230 巷 1 號 2 樓

聯絡電話：(02) 2931-3071

行動電話：0912-598-655



電子信箱：M96520009@mail.ntou.edu.tw

學 歷：

國立台灣海洋大學河海工程研究所碩士 (2007.09 ~ 2008.07)

國立台灣海洋大學河海工程研究所學士 (2003.09 ~ 2007.06)

著作目錄：

(A) 期刊論文

- 1 Chen J. T., Chou K. S. and Kao S. K., One-dimensional wave animation using Mathematica, Computer Applications in Engineering Education, Accepted, 2009.
- 2 Chen J. T., Chou K. H., Kao S. K., Derivation of Green's function using addition theorem, Mechanics Research Communications, Accepted, 2009.
- 3 Chen I.L., Chen J.T., Lee W.M. and Kao S.K., Computer assisted proof of spurious eigensolution for annular and eccentric membranes, Journal of Marine Science and Technology, Accepted, 2009.
- 4 Chen J. T., Kao S. K., Lee Y. T. and Lin Y. J., On the spurious eigenvalues for a concentric sphere in BIEM, Applied acoustics, revised.
- 5 Chen J. T., Kao S. K., Lee W. M. and Lee Y. T., Eigenproblems of a multiply-connected domain with circular boundaries using the multipole Trefftz method, submitted.

(B) 會議論文

- 1 Kao S. K., Lee, Y. T., Lee J. W. and Chen, J. T., On the spurious eigenvalues for a concentric sphere in BIEM, 中華民國力學學會第三十二屆全國力學會議論文集, 中正大學.

(C) 榮譽

- 1 榮獲 97 年度『中興顧問社獎學金』。
- 2 榮獲 96 年國家科學委員會『大專生暑期專題研究』之補助。
- 3 榮獲 95 年中國工程師學會學生分會之『全國學生論文競賽』優等。